

A modelling system for identification of maize ideotypes, optimal sowing dates and nitrogen fertilization under climate change – PREPCLIM-v1

Mihaela Caian¹, Catalin Lazar², Petru Neague¹, Antoanelia Dobre¹, Vlad Amihaesei¹, Zenaida Chitu¹,
5 Adrian Irasoc¹, Andreea Popescu¹, George Cizmas²

¹ National Meteorological Administration Romania (NAM), Sos. Bucureşti-Ploieşti nr.97, Sector 1, 013686 Bucureşti România

² – National Agricultural Research and Development Institute (NARDI) Fundulea, 915200 Călăraşi, România

Correspondence to: Mihaela Caian (mihaela.caian@gmail.com)

10 **Abstract.** Climate change significantly threatens crop yields levels and stability. The complex interplay of factors at the local scale makes assessing these impacts difficult, requiring coupled climate-phenology models, which integrate climate data and crop information. Identifying suitable local management practices and crop varieties under future conditions becomes essential for developing effective adaptation strategies.

This study presents the implementation and application of an integrated climate-phenology adaptation support modelling 15 system. This is based on regional CORDEX climate models and the CERES Maize model from the DSSAT platform. Novel modules for optimal management and genotype identification under climate change have been developed in the system, employing a hybrid approach that combines deterministic modelling with machine learning (ML) techniques and genetic 20 algorithms. This system was run as a regional pilot over Southern Romania, operating in real-time in interaction with users, performing agro-climate projections (combination of fertilization, sowing date, genotype) and providing best crop management simulated under climate change projections. Multi-model ensemble simulations were conducted for two radiative forcing scenarios RCP4.5 and RCP8.5 and twelve management scenarios, yielding novel results for the region. Results indicate a projected decrease in maize yields for the current genotype across all tested scenarios, primarily attributed 25 to a shortened grain-filling period and reduced fertilization efficiency under warmer conditions. Soil initial conditions were found to significantly influence yield responses.

25 The analysis warns about a projected narrowing of the agro-management options for maintaining a high yield level. However, we find an added value from the impact of genotype selection in mitigating climate change impacts, even in extreme years. Genotype optimisation across six crossed cultivar dependent parameters revealed that while maximum yields 30 declines, specific genotype windows exhibit increased intermediate yields under future climates compared to current conditions. Sensitivity analysis identified the thermal time requirements during juvenile and maturity stages as the most critical factors influencing genotype performance under warmer climates.

This research demonstrates the added value of combining deterministic and data-driven modelling approaches within a coupled climate-crop system for developing effective adaptation strategies, including optimised fertilization pathways that contribute to climate change mitigation.

1. Introduction

According to the IPCC (2022), climate change is unequivocal, and its impacts appear more worrying today than decades ago. While research on the effects of climate change on crop yields and agricultural harvests has advanced (Arnell and Freeman, 2021; Hatfield et al., 2021; Rezaei et al., 2024), translating these findings into actionable solutions and scales 40 remains a challenge. This is primarily due to the high complexity of factors that intervene at the local scale of the crop (Malhi et al., 2021; Eyring et al., 2021) including sensitivities of the exchanges to variations in climate sub-components as atmosphere / soil/ biosphere's ecosystems under climate change, natural causes and human activities (Wheeler and Braun, 2013; Xie et al., 2023).

Given the projected global population increase estimated in scientific reports to over 9 billions by 2050 (Godfray and 45 Charles, 2010), global food production would have to increase by 70-100% to meet the growing demand (Smil, 2005; World Development Report, 2008; Selvaraju et al., 2011). This challenge is further compounded by the agro-climatic conditions expected to become vulnerable and gradually decline due to climate change, particularly impacting water availability (Stehr and von Storch, 2009; Villalobos et al., 2012; van Ittersum et al., 2013).

Another challenge of the problem comes from the need that approaches, and sustainable solutions must not only address the 50 needs of agricultural producers but also align with climate change mitigation goals for 2050, aiming for climate neutrality (Semenov and Strattonovitch, 2015; Dainelli et al., 2022; Mitchell et al., 2022).

Early studies investigating the impact of climate change on crop yields emphasized the necessity of high-resolution modelling approaches. These models should accurately represent management practices and the local effects of climate variables, such as temperature and precipitation (McKee et al., 1993; Trnka et al., 1995; Adams et al., 1998). These affect 55 thermal and water stress and plant physiological processes like stem water potential, stomatal opening, leaf transpiration efficiency (Espadafor et al., 2017). At the regional scale, the relationship between crop yield and water and thermal availability may exhibit strong dependencies on the crop type, geographical location, temporal scale, and plant developmental stage (Webber et al., 2018, 2020; Marcinkowski and Piniewski, 2018; Berti et al., 2019; Ceglar et al., 2020; Wu et al., 2021). For instance, simulations conducted by Kothari et al. (2022) in regions with arid climates, indicated for 60 future climate change a significant (~30%) decrease without adaptation, but a potential increase (15%) in corn yields under irrigated or under radiation-based genotype efficient use. These findings underscore the critical need for regional simulations that incorporate phenological characteristics with accurate soil moisture estimates to evaluate the effectiveness of various irrigation strategies under future climate scenarios.

In addition to atmospheric conditions, soil properties significantly influence plant growth. These influences occur through 65 physics-based interactions with climate and through alterations in soil chemical composition. Rising air temperatures have been shown to impact the soil carbon budget, with a decline in soil carbon potentially affecting plant and root processes, biochemical cycles, and species composition (Abhik Patra et al., 2021).

Crop modelling at local, regional and global scale has significantly advanced, enhancing our understanding of crop systems and enabling the simulation and projection of future yields. Studies (Tsvetsinskaya et al, 2001; Tao et al., 2009; Ganguly et al., 2013; Schauberger et al., 2020; Chen and Tao, 2022) consistently project global mean harvest reductions with differences in the regional pattern of climate change impact on crop and harvest (Asseng et al., 2015; Li et al. 2022). Not only projected spatial but also temporal variability of the climate change impact appears larger and accelerated, motivating intensified efforts on seasonal and multi-annual predictions of plant development and harvest (Baez-Gonzalez et al., 2005; Jin et al., 2022). Analysis of these simulations emphasized also the need to include crop uncertainty in climate scenarios assessments (Meehl et al., 2007, Rosenzweig et al. 2013, Basso Bruno et al., 2019; Chapagain et al., 2022).

Meanwhile, model simulations emerged as useful tool in plant breeding analysis (Bernardo, 2002; Banterng et al, 2004; Cooper and Messina et al., 2023; Mamassi et al., 2023), supporting the development of superior genotypes and breeding methods for maximizing crop performance. These simulations have proven effective in guiding cultivar selection through techniques such as parental selection and breeding by design (Peleman and van der Voort, 2003; Qiao et al., 2022).

In most recent years climate-crop modelling extended from deterministic crop models (Boogaard et al. 2013; Morell et al., 2016) to data-driven techniques approaches for assessing crop response to weather and climate change (Schwalbert et al., 2020; Meroni et al., 2021; Morales and Villalobos, 2023; Chang et al., 2023; Zhuang et al., 2024). Statistical methods as well as machine learning (ML) used for crop forecast and modelling were however shown to bring for now, limited benefits (Paudel et al., 2021), pointing to possibly hybrid techniques that include physical process in the modelling as a key approach for this challenging issue. On the other hand, breeding optimization techniques using fully deterministic model simulations require a huge number of simulations, analysis and inter-comparisons of predicted crop performance (Pfeiffer et al., 2007; Wang et al., 2023).

Here we present a novel hybrid approach developed in the frame of the PREPCLIM (“Preparing for climate change”) project in which we solve plant phenology using deterministic modelling and merge this technique with an on-line ML-genetic algorithms (GA) iteratively selecting along simulations the multiple parameter range the cross-range of optimal crop cultivar parameters, according to user-defined criteria for optimal target. The GA simulates the evolution of a population by applying in iterations, genetic operators (selection, crossover, mutation) to a set of candidate solutions (chromosomes). The chromosomes represent potential solutions to the problem and are encoded as strings of binary or symbolic values, with their fitness assessed by a problem-specific evaluation function here, user-required based. GAs have demonstrated success for optimizing agricultural practices using models like DSSAT for irrigation and fertilizer applications (Bai et al., 2021; Wang et al., 2023).

The hybrid approach implemented in this work focused on ideotype identification presents the advantage of physically treating the crop complex process involved along optimizing iterations, thus allowing specific inclusion and understanding of physical causes of responses and of optimal paths in various climate and management scenarios. Furthermore, it enhances the ability of choosing optimum conditions from continuous multi-dimensional intervals for gene parameters, as opposed to discrete sets. The continuum values approach is an important feature mainly for isolated extreme yield detection, or broader

parameters' range and high non-linearity, both aspects of increasing relevance in the context of climate change. Our findings suggest a narrowing of agro-management adaptation opportunities under warmer climates, further emphasizing the importance of this hybrid genotype-agro-management approach to support finding solutions for the future.

105 The developed system aims to provide efficient and operational support for farmers and stakeholders. It leverages the state-of-the art DSSAT model, a widely used and extensively validated platform for agricultural modelling across diverse applications. The DSSAT model, incorporating complex parameterizations for soil processes, surface-atmosphere exchange, plant development stages, and their interactions with climate and management practices, undergoes continuous refinement through ongoing research and regional calibrations. For this study, the model was specifically adapted to the unique soil characteristics of the pilot region, including parameters such as porosity, composition per soil layers, and thermal properties.

110 ~~The developed system exhibits portability to other regions with available soil and management data. Its functionality and user-friendliness are expected to improve through widespread adoption and the incorporation of advanced user requests and management options.~~

115 Section 2 presents the developed system and its data flow. ~~Section 3a provides the motivation for system development, focusing on projected climate change impacts for the target region.~~ Section 3ab presents results obtained using the system to simulate projected changes in plant phenology and crop parameters for the target region, under various climate and management scenarios, for the current control genotype. Section 3be discusses results obtained using the system's genotype optimization package along agro-management scenarios. Finally, Section 4 presents perspectives and conclusions.

2. Data and methods

120 | 2.1 Study region

Recent observations indicate the Southern Romania as being one of the main hot-spots of climate warming in Europe in summer, with high and persistent extreme heat stress and drought being observed (Copernicus report, 2024). Further, projections of climate for the region show an amplification of this response in climate scenarios, mainly in RCP8.5 (suppl. S1.a). For this region, also total precipitation is projected to decrease, while there is an enhancement of extreme precipitation occurrence (suppl. S1.b). These tendencies are increasingly threatening agro-climate conditions in the region, projecting a warmer and drier climate with enhancing extremes.

125 | 2.2 Scientific approach

Projected changes in agro-climatic parameters for Romania were assessed under two Representative Concentration Pathways (RCPs): RCP4.5 and RCP8.5. These changes were computed as anomalies relative to historical simulations (Hist) using an ensemble of three CMIP5-CORDEX (Benestad et al., 2021, Karl et al., 2011) high resolution (11 km) climate models, based on the CNRM, EC-EARTH, and MPI global models coupled to the regional climate model RCA4. Subsequently, the DSSAT crop model (Jones et al., 2003; Hoogenboom et al., 2019) was employed to simulate projected changes in

phenological and harvest parameters. The DSSAT model was driven by atmospheric conditions derived from each model of

135 the ensemble for the historical period and for the two RCP emission scenarios.

A software package was developed for the DSSAT model that performs identification of optimal model parameters based on user-defined: criteria for optimum, climate-management scenario, region, and time horizon. Optimization goals include maximizing harvest, ensuring stable yields over time, and minimizing nitrogen leaching beyond the root zone (reducing 140 water pollution risk). Management scenarios allow users to explore optimal cross-combinations of sowing dates, fertilization amounts, and genotypes.

| ~~Five~~Six main cultivar-specific parameters (P1 to P~~56~~56) characterizing the maize genotype were analysed across wide ranges of physically realistic values, considering both current and extreme future climate projections for the target area. P1 represents the thermal time from seedling emergence to the end of the juvenile phase, ranging in these simulations from 100 145 to 500-degree days above a base temperature of 8°C. It significantly influences crop flowering times (Liu et al., 2020), water availability, and ultimately, yield. Studies have shown that utilizing longer-season maize cultivars (dependent also on P1) can lead to increased harvest in humid regions but decreased harvest in semi-humid regions (Mi et al., 2021).

| P2, a photoperiod sensitivity parameter, represents the extent to which development (expressed in days) is delayed for each hour increase in photoperiod above the photoperiod of maximum development rate (which is considered to be 12.5

150 hours), is ranging in simulations here from 0.1 to 2.6 days. Or: Longer days increase the period of plant development only up to a threshold value, here 12.5 hours. P2 measures (in days) the delay in plant growth for each hour of photosynthseys above this threshold.

P2 influences the flowering time (Langworthy et al. 2018) and the rate of plant development, with long-day plants exhibiting faster development under longer day lengths (Angus et al., 1981). Related to these, studies have demonstrated the significant role of P2 in mitigating the negative impacts of waterlogging in warmer climates (Liu et al., 155 2023). P3, the thermal time from silking to physiological maturity, here tested for values from 500 to 1500-degree days above a base temperature of 8°C, significantly influences maturity dates. It also has a main role in plant stress levels (longer-maturity hybrids increase harvest but under water stress it may provide lower yield (Su et al., 2021; Grewer et al., 2024)) and grain moisture at maturity (Tsimba et al., 2013). P4, representing the maximum number of kernels per plant, exhibits a relatively predictable numerical response and is therefore held constant at the control value of 797.5 estimated for the region, in this analysis.

P45, the kernel filling rate parameter (ranging from 6 to 12 mg/day), influences grain filling duration, desiccation, moisture at maturity and harvest (Chazarreta et al., 2021). P~~56~~56, the phyllochron interval, the interval in the thermal time (degree-days) between successive leaves tip appearances (expressed in degree-days above a base

temperature of 8°C, ranging in these simulations from 3 to 70 °C-days), is a critical parameter for estimating the duration of vegetative development (Birch et al., 1998; Xu et al., 2023). P~~5~~5P~~4~~4 and P~~56~~56 are important parameters of optimal plant

160 adaptation to climate conditions, since they are drivers of the phenological response and yield formation, in conjunction with the temperature, radiation, humidity, water stress. These genotype (or cultivar specific) parameters are the primary ones considered in DSSAT model parameterizations for plant development processes (Hoogenboom et al., 2019).

170 The parameter ranges were rigorously tested in simulations to ensure their representativeness for the target region, including and to allow further analysis of extreme values. The control values for these cultivar-specific parameters P_i in the region are: $P1=200$, $P2=0.7$, $P3=800$, $P4=797.5$, $P45=8.60$, and $P56=38.90$. All the simulations for combinations of parameters values (cross-parameter P_i simulations) were performed under Hist, RCP4.5, and RCP8.5 emission scenarios. For each scenario, crop projections simulations were conducted for twelve agro-management scenarios (Table 1) consisting of sowing date changes and fertilization treatments, characteristic for region after the year 2000 (Table 1a), for each model of the ensemble. Then, for the genotype sensitivity simulations e.g. the response to genotype, optimal genotype selection we have chosen a lower fertilisation (Table 1b), already used in the region before the year 2000 (when the number of subsistence farms was high), value aimed for potential mitigation (Ursu, 2025), in potential synergy with genotype selection. It was shown that Romania, with a consumption of 46 kg/ha, had an efficiency comparable to countries with much higher consumption, indicating a significant potential for improvement without increasing environmental pressure (Ursu, 2025).

180 In the platform, By default, the twelve agro-management scenarios encompass four sowing dates (spaced five days apart) and three fertilization levels (zero, then a regional average and its double, Table 1a). For each agro-management scenario, genotype optimization (finding the optimal set of parameters P_i values under the given climate -agro-management and optimum criteria) was performed using two methods: 1) discretized parameter-space runs with subsequent post-processing ordering, and 2) continuum parameter-space search with iterative selection during simulations, employing genetic algorithms (GA). The

optimization is performed for each year, allowing the optimal management and cultivars to evolve over time, and also allowing further investigations of response e.g. during critical years or in clusters of climate conditions, or as ensemble time-mean.

190 The proposed GA-based method employs an iterative approach. It commences with an initial population of randomly generated solutions (chromosomes) and undergoes iterative cycles (generations). In each generation, a selection process is performed to choose the fittest chromosomes for reproduction, based on their fitness scores. Subsequently, crossover (recombination) and mutation operators are applied to the selected chromosomes, generating offspring that inherit traits from their parents. The new offspring replace some of the least fit individuals in the population, ensuring that the average fitness of the population improves over time. The convergence of the GA toward an optimal or near-optimal solution is achieved by balancing exploration (searching the problem's space for diverse solutions exploiting promising regions) and exploitation (refining the best solutions found so far).

2.3 The Software

200 Here GA has been newly applied to develop an innovative crop selection algorithm, optimizing genotypes across various agro-management scenarios. Steps along the algorithms are described in Annex. workflow of ML algorithms for optimal genotype identification are:

1. Start with 10 randomly chosen solutions within the bounds of P1-P5;
2. Calculate the mean and standard deviation of harvest of each solution for the 30 years 1976-2005;
3. Calculate fitness = (mean of harvest) – (standard deviation of harvest)/4;
4. Randomly choose 4 pairs of ‘parents’, with the probability being chosen weighted by the fitness;
5. For each pair of parents A and B, create identical children ‘a’ and ‘b’ to the parents, then choose a random number of P’s to be subjected to crossover, called x;
6. For each child, modify Px as follows:

210
$$P_{xa} = \text{round}(B * P_{xa} + (1 - B) * P_{xb});$$
$$P_{xb} = \text{round}((1 - B) * P_{xa} + B * P_{xb})$$

215 7. Where P_{xa} is the value of the x parameter of child “a” (initially identical to that of parent A), and B is the blending factor, set in this paper to 0.75. This technique is called blending, and it generates offspring chromosomes that inherit real-valued traits from both parents while exploring the search space between the parents' positions. The blending crossover promotes a smoother and more gradual search for optimal solutions in continuous domains.

8. Then take each child, and with a probability of 0.5 perform a mutation on one of its chromosomes. This means setting one of the P’s to a random value between its allowed minimum and maximum.
9. At this point the children have been fully constructed. Discard the 8 parents with the lowest fitness and substitute them with the children.

220 10. Repeat from 2.

225 The system generates output data (agro-climate and optimal paths of cultivars and agro-management) which is disseminated on two platforms (Fig.1). One is a platform (Info-Platform, Fig.1a) providing one-way interactive (static) agro-climate information at local scale (NUTS3 level, aligned with the European Union's Nomenclature of Territorial Units for Statistics, primarily corresponding to county level in Romania) over the region. It delivers pre-computed regional climate and agro-climate indicators (e.g. drought, soil moisture, evapotranspiration, aridity indices, storminess, model-based phenological dates, yield), indices of agro-climate extremes (e.g. extreme precipitation frequency and intensity, extreme temperature, scorching index, wind gust, number of freezing / icing days, diurnal temperature range, biological effective degree days) based on observations, re-analysis and climate scenarios for future projections for the region.

230 The second platform (User-Platform, Fig.1b) is an operational, online, user-interactive (two-way) in real-time component, where user requests are submitted, processed as input to the modelling chain and results delivered back to the user for a new, refined request.

The core of the modelling system integrates the DSSAT crop model (running on Linux OS) with regional climate models (Fig.2), with a pre-processing pack developed for coupling. This coupled system incorporates new features, that include the 235 ability of conducting parameter-varying cross-simulations and advanced algorithms for identifying optimal agro-management practices and genotype selections along simulations.

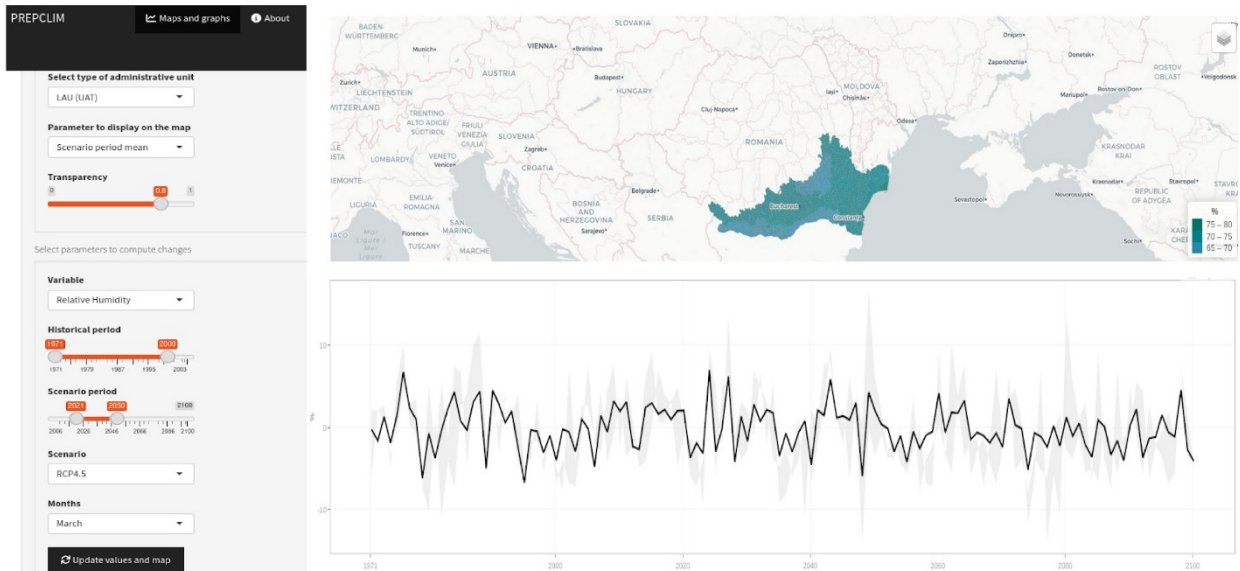
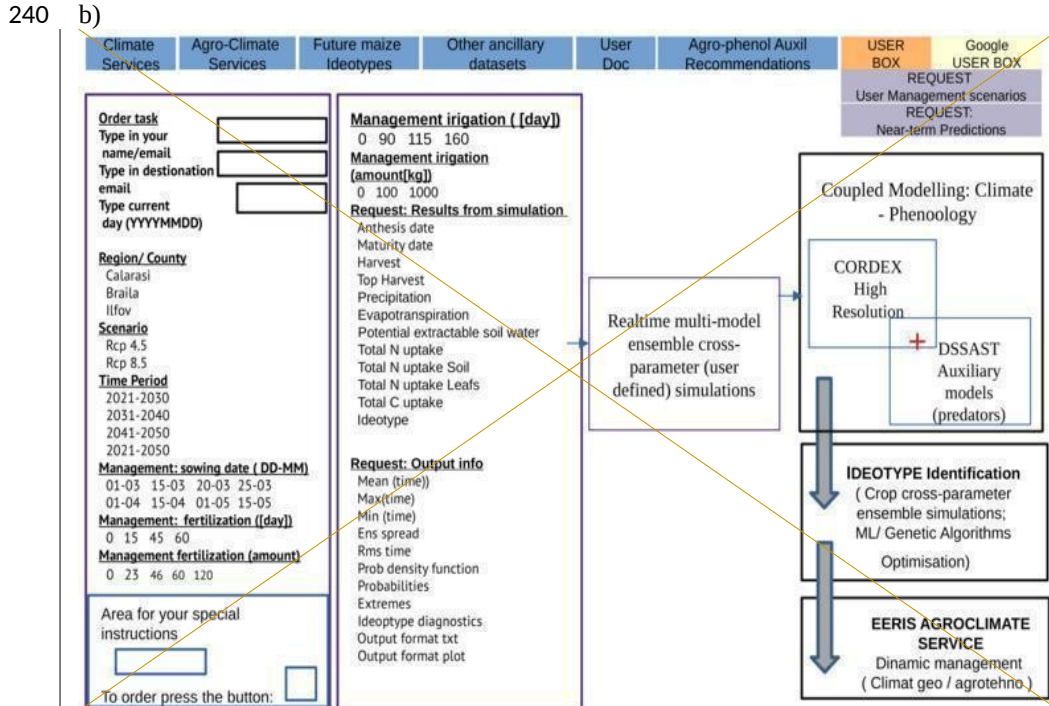
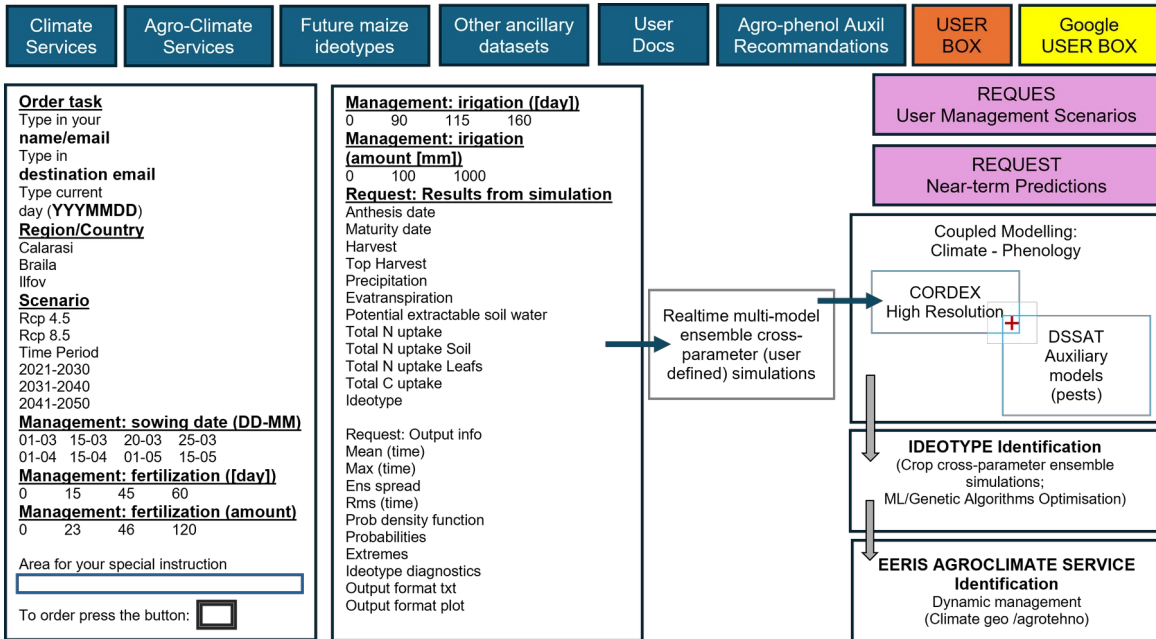


Fig.1 a): Info-Platform: Provides local-regional scale information derived from high-resolution regional climate models (CORDEX), e.g. climate, agro-climate data and indicators, indices of agro-climate extremes at the NUTS3 level.

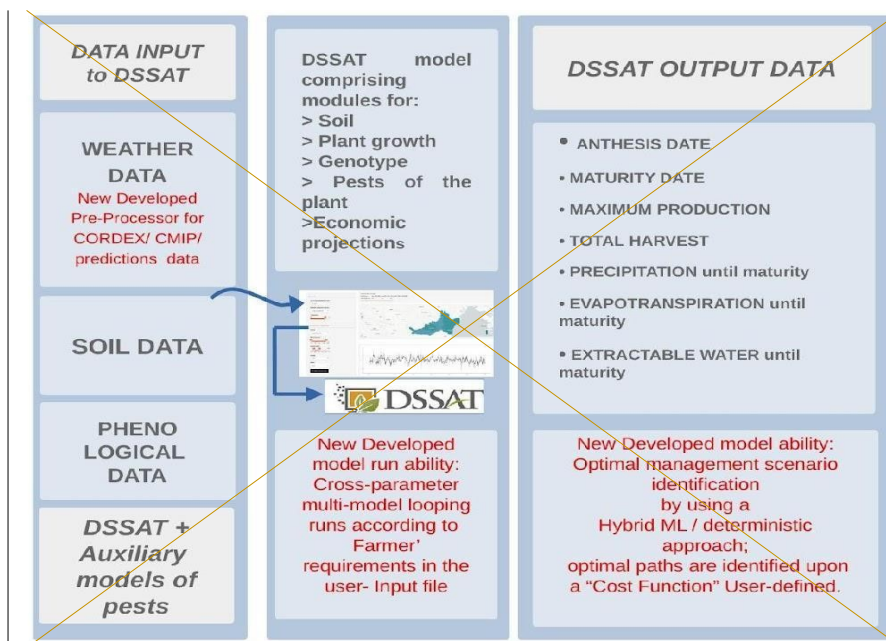


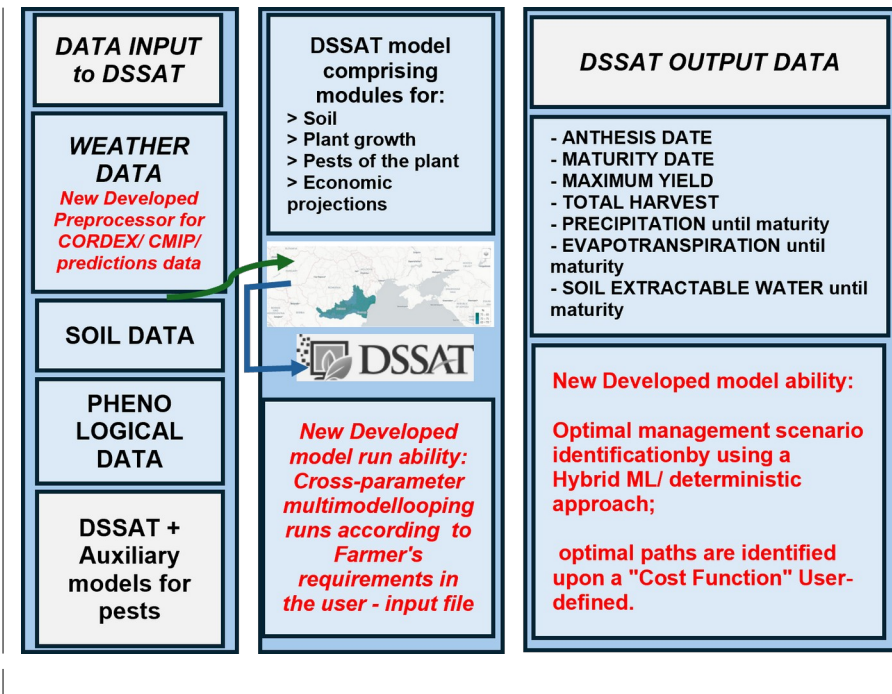


245

250

Fig.1 b): User-Platform for adaptation support: Processes in real time specific user requests, and simulates management scenarios, identifying optimal paths: Users input parameters (left, e.g: region, period (present / future climate scenarios), management options (e.g. sowing date, fertilization/irrigation time and amount, genotype); System Output (right, e.g: harvest, projected phenology dates, precipitation/evapotranspiration, Nitrogen and carbon balances, optimal management paths (dates and management actions), optimal genotype) estimated from ensemble simulations.





255

260 Fig.2: The PREPCLIM-v1 work schema: DSSAT-core and modelling components (middle), and data flow: input data (left), output information (right). Red modules were developed in PREPCLIM-v1.

The system was implemented and validated over Southern Romania, target agricultural area, for maize. Potential beneficiaries include researchers, farmers, policymakers, and maize breeders. The system can also assist maize breeders in adapting to climate change by enabling them to evaluate and select genotypes more resistant to challenging climatic 265 conditions. Given the accelerating pace of climate change, such a system may provide valuable support in numerous ways.

270 **Table 1: The agro-management treatments:** each treatment is described in terms of the sowing date and Nitrogen fertilization amount, Nitrogen [kg/ha]. We denote two experiments: exper “1N” and exper “3N”, and fertilisations Fx0, Fx1, Fx2 have values dependent on the experiment: In function of the experiment type: a) the experimental set-up for crop phenological projections has: Fx0=0 (is no fertilisation), Fx1 (the regional average fertilization after the year 2000, 60 kg/ha) is the unit fertilisation of the experiment and Fx2 (is the double of Fx1, 120kg/ha) unit fertilisation of the experiment. We define the unit fertilisation of the exper “1N” equal to 23 N/kg and the unit fertilisation of the exper “3N” as 60 kg/ha, for each treatment (TR); b) the experimental set-up for genotype optimisations has: Fx0=0, Fx1=23; Fx2=46 kg/ha, values used before 2000, for each treatment (GTR). Sowing date format is “DD.MM”

a) The experimental set-up for crop phenological projections

Treatment	TR1	TR2	TR3	TR4	TR5	TR6	TR7	TR8	TR9	TR10	TR11	TR12
Sowing date	1.04	15.04	1.05	15.05	1.04	15.04	1.05	15.05	1.04	15.04	1.05	15.05
Fertilization (exper “3N”)	Fx0 =0	Fx0	Fx0	Fx0	Fx1= 60	Fx1 =60	Fx1= 60	Fx1= 60	Fx2 =120	Fx2 =120	Fx2 =120	Fx2 =120
Fertilization (exper “1N”)	Fx0 =0	Fx0	Fx0	Fx0	Fx1= 23	Fx1 =23	Fx1= 23	Fx1= 23	Fx2 =46	Fx2 =46	Fx2 =46	Fx2 =46

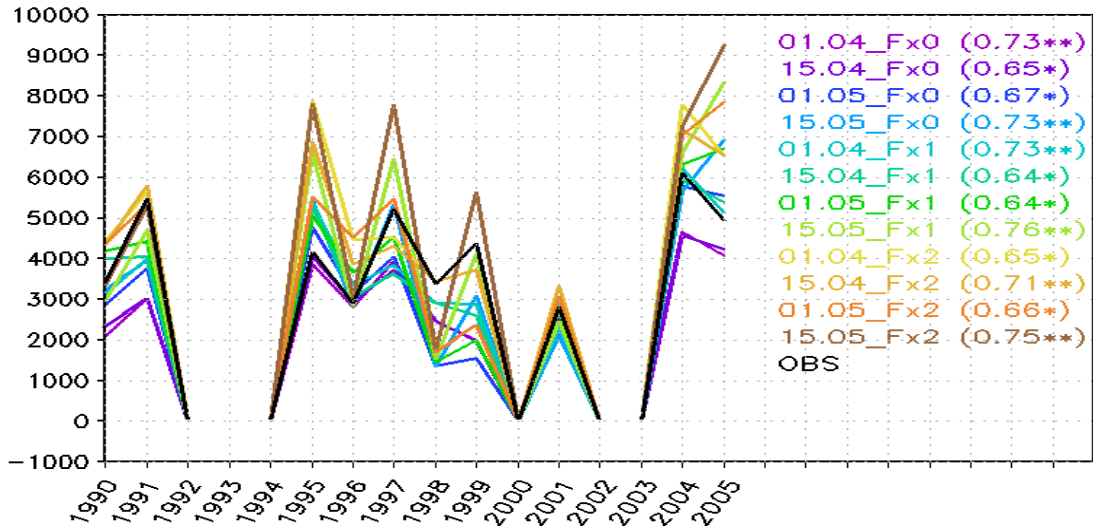
275 b) The experimental set-up for genotype optimisation

Treatment	GTR1	GTR2	GTR3	GTR4	GTR5	GTR6	GTR7	GTR8	GTR9	GTR10	GTR11	GTR12
Sowing date	1.04	15.04	1.05	15.05	1.04	15.04	1.05	15.05	1.04	15.04	1.05	15.05
Fertilization (exper “3N”)	GFx0 =0	GFx0	GFx	GFx0	GFx1 =23	GFx1 =23	GFx1 =23	GFx1 =23	GFx2 =46	GFx2 =46	GFx2 =46	GFx2 =46

3. Results

3.1 Model validation

Model validation was conducted using Control simulations (Ctrl) driven by ERA5 reanalysis data (Simmons et al., 2021) for each treatment outlined in Table 1a. These simulations, spanning the period 1976-2005, demonstrate the model's ability to capture inter-annual variability in harvest yields, including both high and low yield years, when compared to the measured available data for the region (Fig.3). The amount is more challenging for validation due to time-evolving constraints over the region. Some contributions were identified, as large variations in fertilization over 1990-2000 with an abrupt decay after 1991, then followed by an increase around 2000 (Popescu et al, 2021), variations in the work practices, pest and willing and lack of countering methodology. However these are traceable in these simulations' comparisons (with lower skill about 1995, for which it was reported a minimum of sowing effective (INSP, 2022, suppl. S2) and a mximum of wilig (ref)).



290 **Fig.3: Simulated (colors) vs. measured (black) harvest in southern Romania for 12 management scenarios (Table 1a). Right: treatment defined by sowing date and fertilisation (Table 1a) and Pearson correlation between simulated treatments and measured Harvest (** p<0.01, ** p<0.05, * p<0.10; zero are missing values).**

3.1 Agro-climate changes in the region

295 3.1.1 Climate changes in agro-climate indicators

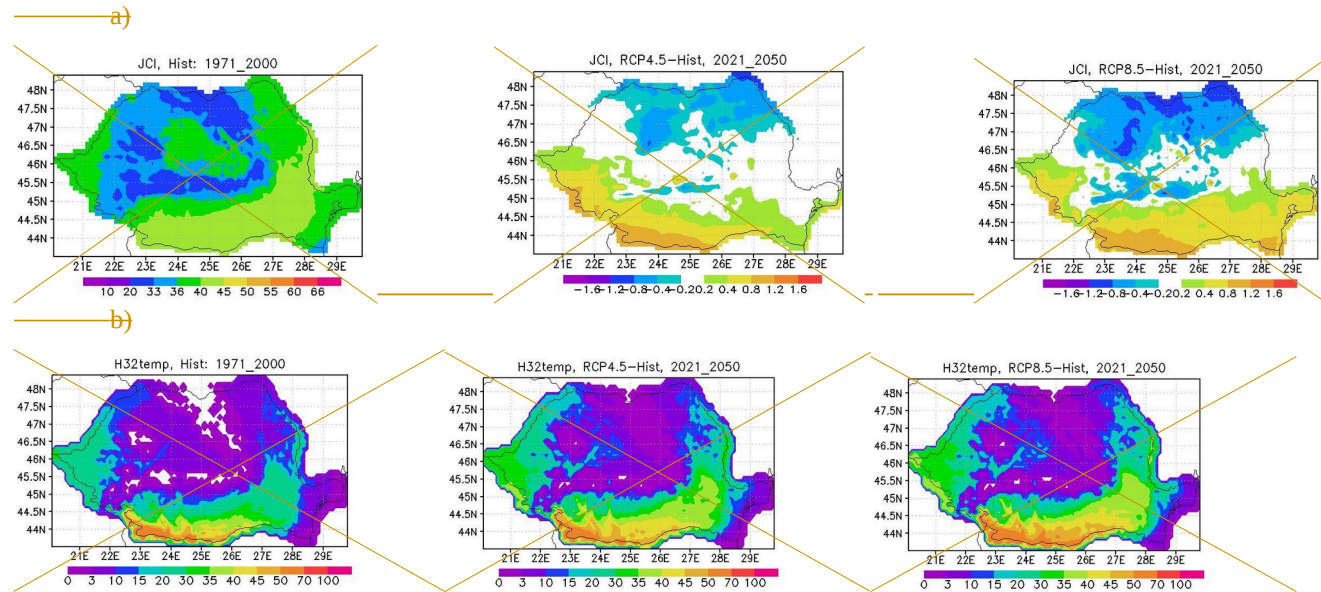
Agro-climatic Indicators, derived from CORDEX models and available on the Info-Platform, provide time-series data for ensemble or individual model metrics at the NUTS3 level across Romania. Figure 3 illustrates projected changes in key agro-climatic characteristics.

300 The anticipated climate shift in the region is evidenced by changes in the Johansson Continentality Index (JCI, Fig.3a), calculated as $JCI = 1.7 * dT / \sin(\phi) - 20.4$ (where dT is the annual maximum range of monthly mean temperatures and ϕ is latitude; (Flocaș, 1994; Baltas, 2007)). Changes in the JCI generally reveal robust evidence of large-scale changes influences on the regional climate. For this domain it shows a Southwards meridional gradient of the intra-annual variability (Arctic amplification remote impacts on Europe). Hence enhanced intra-annual variability (JCI) with much warmer summers than winters over the main agricultural areas in South (and the opposite in the North), information useful for farmers to estimate changes in the sowing time.

305 In agreement with this, the Scorching Index ($H32temp$, Fig.3b, computed as the total degrees in summer days exceeding $32^{\circ}C$), used by farmers and agro-meteorologists to characterize the sub-regional drought conditions, projects severe drought conditions ($H32temp \geq 51$), about doubling the $H32temp$ values and expanding significantly across the southern regions in RCP8.5 with already high-level drought conditions ($31 < H32temp < 51$) occurring in RCP4.5 (Fig.3b).

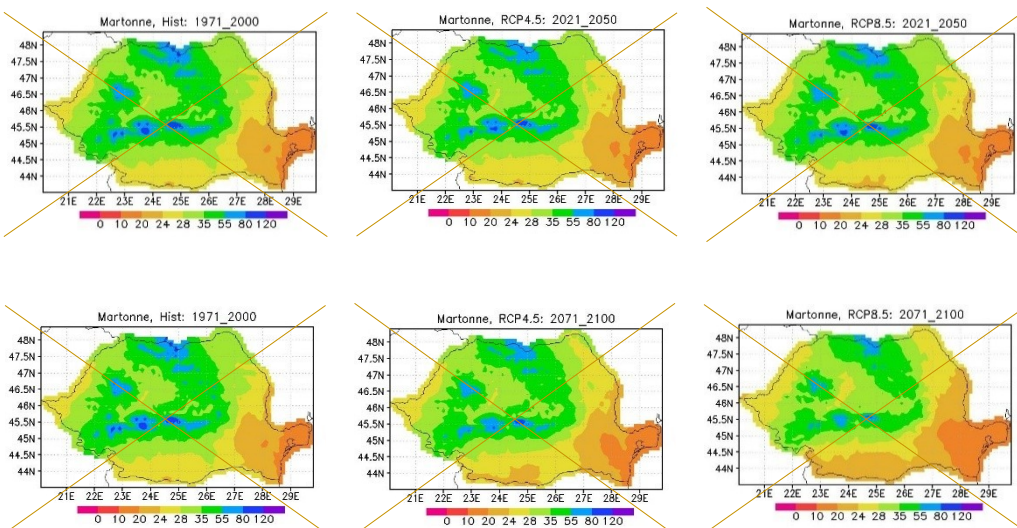
310 Accounting also for precipitation changes, the de Martonne Aridity Index (IM, the ratio of annual precipitation to a translation function ($+10^{\circ}\text{C}$) of the annual mean temperature), exhibits also significant projected changes. It shows particularly increased aridity (low IM) in the south, southeast, and southwest regions, the major agricultural areas with an accelerating change up to 2100 (Fig.4, comparing projected differences to Hist for 2071-2100 versus 2021-2050).

315



320

Fig.3: The JCI and the Scorching index H32temp indices. For each: (left): the index over Hist period 1971-2000 and changes (2021-2050) relative to it, under RCP4.5 (middle) and RCP8.5 (right). a) The JCI climate index classes are: marine for $0 < k \leq 33$, continental for $33 < k \leq 66$ and exceptionally continental for $66 < k \leq 100$. b) The Scorching index H32temp classes are: reduced intensity drought for $H32temp \in [0,10]$, moderate intensity for $H32temp \in (10,30]$, high intensity for $H32temp \in (30,50]$ and severe drought conditions for $H32temp > 50$.

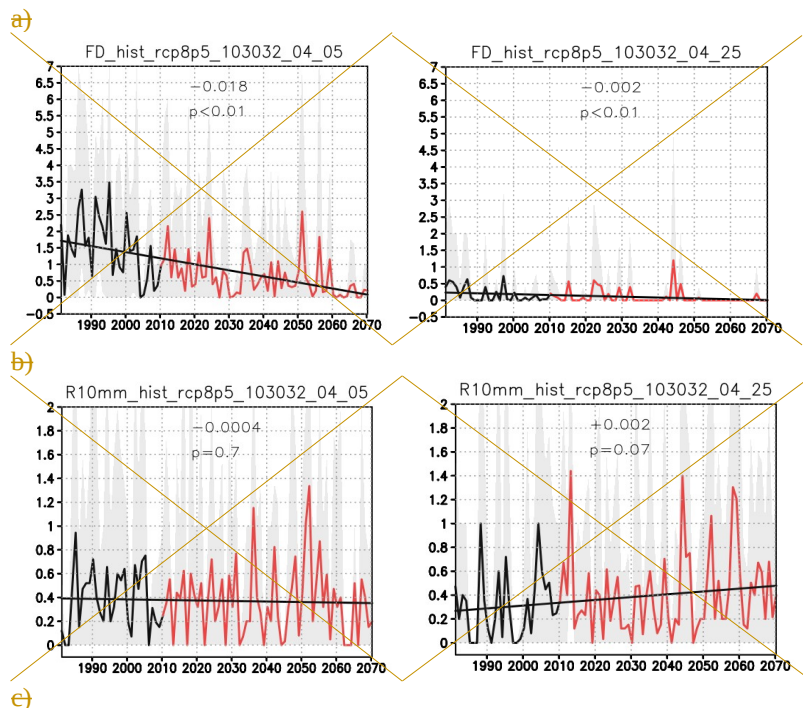


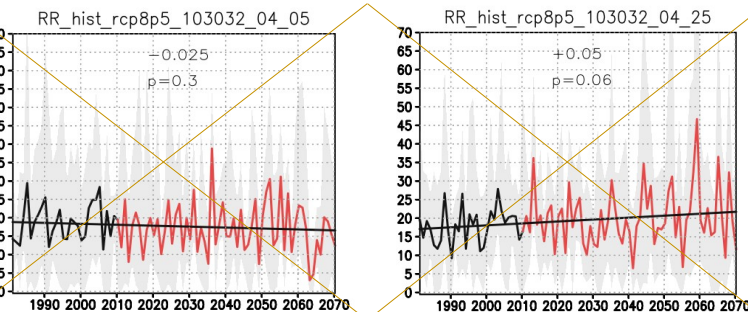
325 **Fig.4: The de Martonne aridity index (IM) for: Hist (left), RCP4.5 (middle) and RCP8.5 (right) for two horizons: 2021-2050 (top) and 2071-2100 (bottom). IM index classes are: arid for $0 < IM \leq 10$, semi-arid for $10 < IM \leq 20$, Mediterranean for $20 < IM \leq 24$, semi-humid for $24 < IM \leq 28$, wet for $28 < IM \leq 36$, very wet for $36 < IM \leq 55$ very wet and extreme wet for $IM > 55$; (all indices are time mean 30 years; ensemble mean).**

3.1.2 Changes in agro-climate extremes

330 Projected changes in extremes for temperature and precipitation, highly useful information for agriculture, show important features in the region. A main aspect of interest is related to late-spring freezing days that may drastically affect the whole crop of the year. Fig.5a shows for South Romania (Călărași subregion) that in spite of the decreasing trend (5% p-level significance) of the total number of freezing days in spring, we still may have severe events with interestingly, a number of freezing days in late-spring that is even higher in scenarios than in Hist, late spring being one of the most vulnerable period to freezing for the plant already under development. Also note that successive extreme freezing years in late-spring may occur.

335





345 **Fig.5: Extreme climate parameters (NUTS region 103032, representative for the target region), along historical (Hist) and RCP8.5 scenarios; a): FD, the number of frost days (minimum temperature < 0°C in a 10-day period); b): RR10, the number of days with heavy precipitation (>10 mm per day) in a 10-day period; c): RR, total precipitation (mm) per 10-day period; (left): the 10-day period is centred on April 5th; (right): the 10-day period is centred on April 25th. Values indicate the slope of the linear trend (black line) and the p-value of significance (p-values < 0.05 are statistically significant at the 5% level).**

This late spring blizzard feature over the region, was analysed in a previous work and shown to be related to the combined context of Polar Jet instability meanwhile with warmer sea surface temperature in the Eastern Mediterranean (Caian and Andrei, 2019). Both these features are projected to enhance in a warmer climate (Lelieveld et al., 2012; Shaw and Miyawaki, 2024), indicating higher potential for severe late-spring blizzards in the region.

355 **For precipitation, analysis of extreme precipitation events (RR10mm) and total precipitation (RR) reveals a notable shift in their temporal distribution within April. While a decreasing trend is observed in the first dekad, a positive trend emerges in the third (and second, not shown) dekades (Fig.5b). These suggest a time-shift tendency towards the end of April and into early May for the occurrence of intense and accumulated precipitation. Although statistically insignificant at the 5% level, this shift is consistently observed across all models within the CMIP5 ensemble. As for FD we note that higher extreme values of RR and RR10 are projected to occur under emission scenarios than Hist, mainly in RCP8.5 (Fig.5b,c), more often during late spring. Extreme daily precipitation is, in most cases detrimental for the crop, causing soil erosion and surface runoff mainly after drought periods.**

3.2 Phenology and Harvest Projections for the Control Genotype

360 Projected changes in phenology for the control genotype (Pioneer 375) were simulated using the DSSAT model under historical (Hist) and multi-model climate projections of ~~E~~RCP4.5 and RCP8.5 scenarios. Further, multi-genotype simulations are discussed in Section 3.3e.

Model validation was conducted using Control simulations (Ctrl) driven by ERA5 reanalysis data (Simmons et al., 2021) for each treatment outlined in Table 1 (experiment "3N").

365 These simulations, spanning the period 1976–2005, demonstrate the model's ability to capture inter-annual variability in harvest yields, including both high and low yield years, when compared to the measured available data for the region (suppl. S1). They also allowed model set-up improvements through sensitivity simulations and model calibration including soil parameters (suppl. S2) as soil water, nitrogen, and organic carbon content.

370 However, further improvements in model accuracy are to be achieved if incorporating factors such as inter-annual soil variability, the yearly impact of pests and diseases or the year-to-year variations in practices of fertilization and sowing dates. For example, simulations with fertilization specifications closer to the year's management practices (e.g. approximately 80–120 kg N/ha and sowing around April 15th for 1995) resulted in more accurate (reduced bias) predictions

(TR6, TR10). These, together with the well simulated inter-annual variability, demonstrate the model's ability to capture the combined influence of climate and management practices on crop performance.

375

3.2.1 Phenology dates - projected changes

Ensemble model simulations provide projected changes in phenology, for the control genotype (G0), under different fertilization levels (0, 60, 120 kg/ha, Table 1, exper "3N") and sowing dates, averaged over 30-years, in scenarios (2021-2050, RCP4.5 and RCP8.5), versus Hist (experiment set-up "E_3N_G0"). Figure 6a,b illustrates the ensemble model changes, demonstrating an earlier anthesis date by up to ~6 days and an earlier maturity date by up to ~10 days across all scenarios. These time-shifts result in a shortening of the grain-filling period by up to 10% across the ensemble, and are a consistent response observed in each individual model. Early sowing dates exhibit a more pronounced earlier shift in anthesis under warming scenarios, a response even more pronounced under RCP8.5.

Under warmer climates we note more frequent occurrences of critical situations with suboptimal grain filling and potential crop failure, under fertilization. These were linked in previous studies to non-linear interactions between fertilization and temperature (Huang et al., 2024) with excessive fertilization during reproductive stages under elevated temperatures potentially inducing higher stress conditions. In our study premature ending of simulated vegetation season occurred more frequently in treatments with higher nitrogen fertilization, leading in average only small changes in maturity days. This may favour leaves development, enhanced transpiration and earlier depletion of the soil moisture leading later to water stress.

390

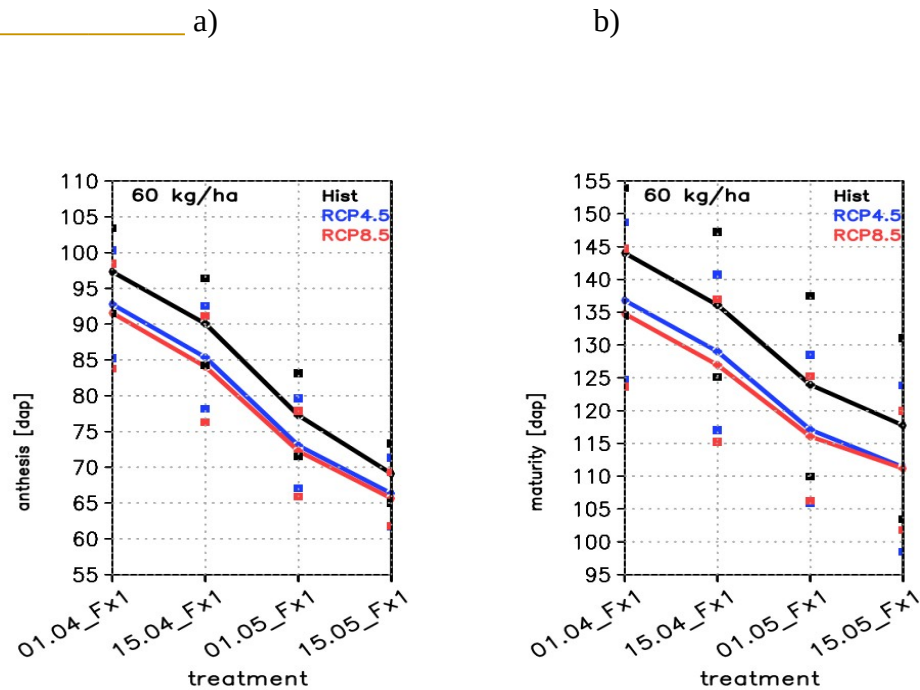


Fig.6 **Fig.4:** Simulated a): anthesis dates ([dap], days after sowing) and b): maturity dates ([dap]), under historical conditions (black), RCP4.5 (blue), and RCP8.5 (red) scenarios, experiment setup E_3N_G0. Results are shown for the four sowing dates and nitrogen fertilization level of 60 kg/ha (Table 1, exper “3N”). The maximum and minimum value over the ensemble members for each treatment and climate is shown (dots).

3.2.2 Harvest - projected changes

For harvest, the ensemble simulations (along E_3N_G0) project an overall decrease under both RCP4.5 and RCP8.5 scenarios and across all sowing dates and fertilization levels (Fig.7Fig.5), compared to the historical period.

Harvest decline in climate scenarios is related to several factors: 1) reduced rainfall during the growing season (Fig.8Fig.6), as evidenced by a strong correlation (0.5 in April to 0.8-0.9 in July-August, over 30 years, suppl. S2) found between harvest (H) and accumulated precipitation in the Ctrl and in model simulations; 2) a shortened grain-filling period due to a projected earlier flowering and an even earlier maturity across all the models (Fig.6Fig.4), potentially limiting biomass accumulation; and 3) decreased fertilization efficiency under warming conditions, in the sense that the H difference of harvest in Hist versus in scenario Hist minus scenario, increases (non-linearly) with enhanced fertilisation (Fig.7Fig.5). Hence for a same climate, the same increase in fertilisation brings less benefit in a warmer climate. This benefit for H is of about 10% in Hist versus 7.6% in RCP8.5 for early sowing and about 8% in Hist versus 4.3% in RCP8.5 for later sowing for doubling the N amount of nitrogen (Fig.7Fig.5b,c). This efficiency decay feature underscores the primacy of reduced accumulated precipitation (Fig.8Fig.6) and of higher temperature, that lead to a non-linear H response to fertilization (Huang et al, 2024). Their influence is noticed as well in the absence of fertilization (Fig.7Fig.5a), when H still declines in warmer climates, with a dominant control from precipitation. The correlation along sowing dates between H and accumulated precipitation until maturity (Pmat, Fig.8Fig.6), is $r(H, Pmat) > 0.96$ in both scenarios.

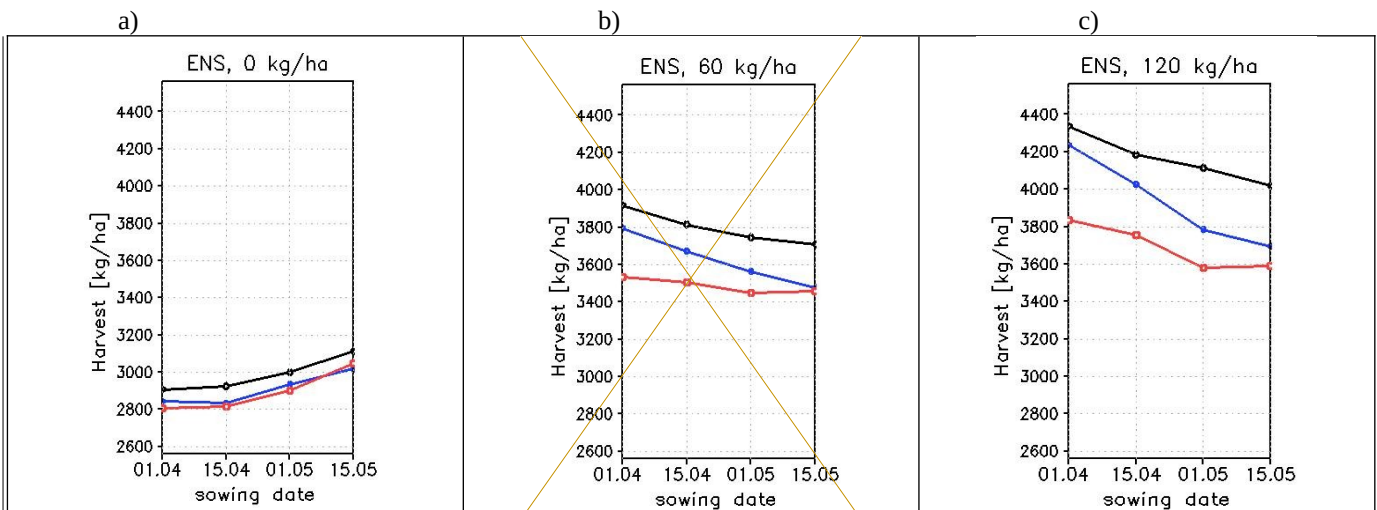


Fig.7E: Simulated Harvest (kg/ha) under Hist (black), RCP4.5 (blue) and RCP8.5 (red) scenarios, for four sowing dates across three fertilization levels (Table 1, exper “3N”): 0 (a), 60 (b), and 120 (c) kg N/ha (from left to right), experiment setup E_3N_G0.

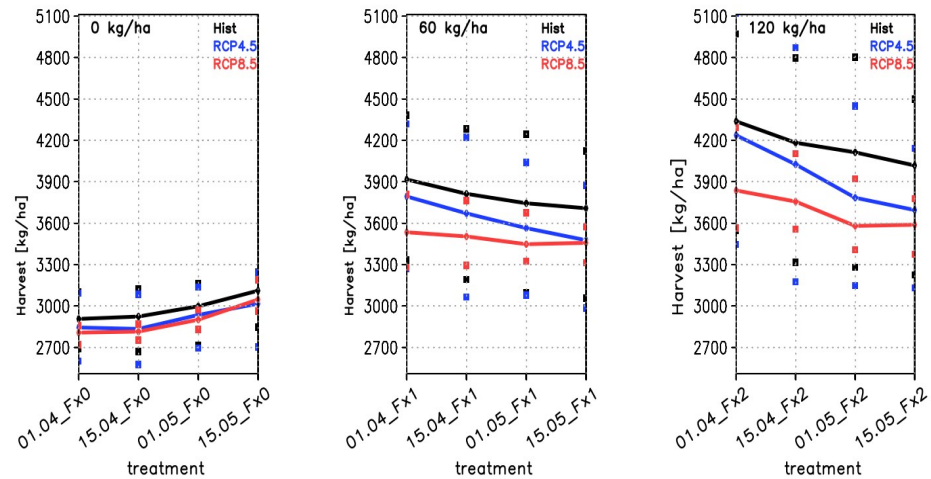
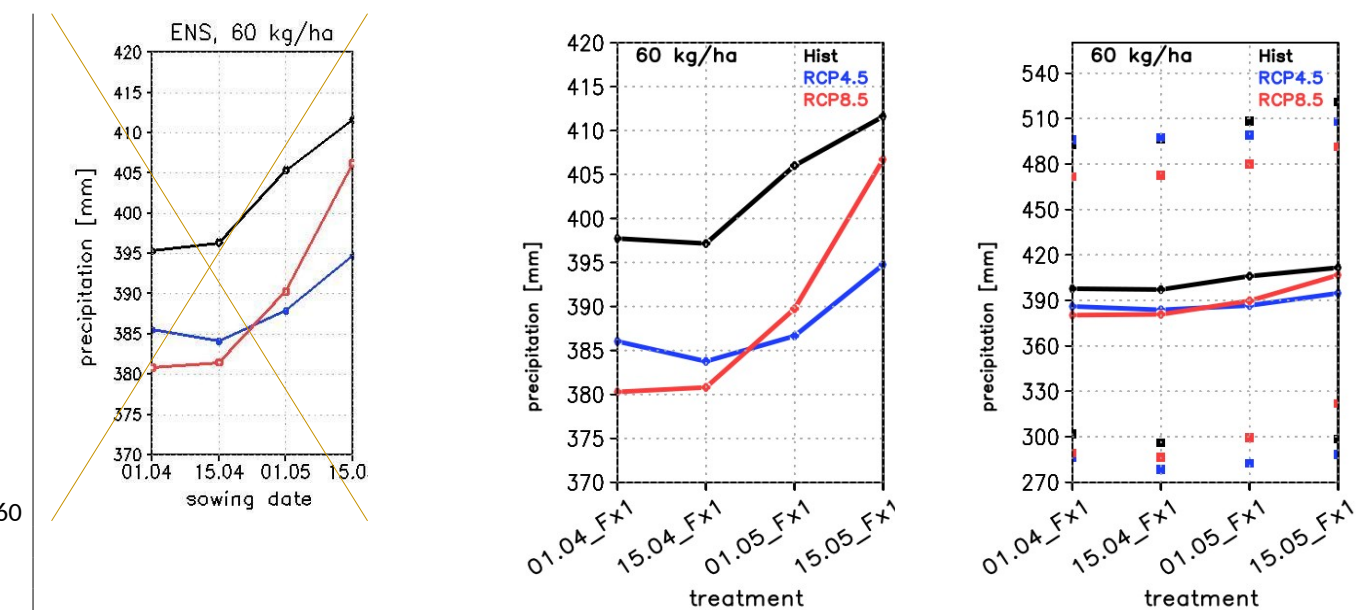


Fig.5: Simulated Harvest (kg/ha) under Hist (black), RCP4.5 (blue) and RCP8.5 (red) scenarios, for four sowing dates across three fertilization levels (Table 1, exper “3N”): 0 (a), 60 (b), and 120 (c) kg N/ha (from left to right). The maximum and minimum value over the ensemble members for each treatment and climate is shown (dots).



470 **Fig.8Fig.6: Precipitation accumulated until maturity (mm) in experiment E_3N_G0 (legend as in Fig.5-7). The maximum and minimum value over the ensemble members for each treatment and climate is shown (dots).**

475 The role of the precipitation timing is emphasised: for late sowing, RCP8.5 shows more accumulated Pmat (and H) despite a shorter accumulation season (Fig.6Fig.4) but having projected a precipitation increase towards late spring (Fig.S1b5), that may significantly favour critical growth stages.

3.3 Optimal Genotype Identification

480 The system was further developed to extend the management scenarios for multi-genotype simulations and implement methods to identify ideotypes under each agro-climate scenario. The aim is to search for management scenarios that yield optimal outcomes defined by user-criteria such as maximizing harvest yield, stabilizing yield, or minimizing pollutant emissions. Two optimization methods are implemented: a discrete-parameter, purely deterministic technique, and a hybrid approach that combines deterministic modelling with continuous-parameter Machine Learning-based Genetic Algorithms for iterative genotype selection.

485 The deterministic method involves conducting multiple-genotype crop model simulations, with optimization performed as a post-processing step. Genotype parameters P_i are defined within pre-established limits and discretization. Multi-model simulations are then performed, where each parameter is individually varied while the remaining parameters are held constant. The total number of simulations in this case is determined by the chosen discretization level. In contrast, in the hybrid technique the P_i values are selected from a continuous range of values, identifying and iteratively improving the best sub-domains. This section presents the results of genotype optimization experiments (E_1N_Gn+w), built upon the E_1N_G0 and sets up initial (1st of January, yearly) soil moisture as best agreement with projections targeting 490 near-term (2035 as centre of interval 2021-2050).

3.3.1 Optimal genotype under climate change

i) harvest as a function of the genotype H(G) in scenarios versus current climate

495 We analyse the distribution of H obtained along multi-genotype simulations, ordered from maximum to minimum values and denote the genotypes corresponding to this ordering “H-ordered genotypes”, chain which is simulation (model, scenario) dependent. Comparing these H distributions for the two climate scenarios against Hist, indicates projected changes in the ensemble-model PDF (probability density function) of H under warmer climate.

A first outcome demonstrates in Fig.9Fig.7a, b that for the H-ordered genotypes, a projected average decrease in Harvest (H) occurs within the range of maximum H values (genotypes in the topupper H-percentile interval; interval GX(0%, 2.5%) of the H-ordered genotypes), under both scenarios, and mostly affecting the earlier sowing dates (Fig.9Fig.7b). Across models 500 of the ensemble, we note a strong modulation of this behaviour by precipitation, particularly for unfertilized scenarios. Precipitation exhibits high inter-model variability and significant regional-scale uncertainty, pointing to the need of ensemble modelling for reducing it. In contrast, the warming trend is a consistent feature across models in the region, contributing other model-systematic responses such as earlier anthesis and maturity dates and shortening of the grain filling season.

505 The second note regards a different response projected in the intermediate H values (Fig.9Fig.7a, c). Genotypes corresponding to the intermediate H values (genotypes of intermediatemiddle H-percentile interval, the interval GI (25%, 70%) of the H-ordered genotypes) show projected higher H values in GI in climate scenarios than in Hist (Fig.9Fig.7c), affecting less the earlier sowing (Fig.9Fig.7c).

510 These together lead to a narrowing of the H-values range of responses, in the top and intermediate H-percentile intervals GX and GI, to the same managements applied, in scenarios compared to Hist. Same management spread would lead to closer H- responses, with enhancing the expectancy for occurrence of intermediate values and decreasing the expectancy for highest H values (a third feature of projected changes).

515 Finally, we note that despite this narrowing, earlier sowings appear systematically as better timing options (Fig.9Fig.7a), improving by up to 2%-(4)% in scenarios (respectively to 4% in Hist) unfertilized case and up to 8%-(12)% in fertilised case in scenarios (respectively to 12% in Hist) (Fig.9Fig.7a), with the lowest percentage for RCP8.5. Earlier sowing was reported in other recent studies as optimal for spring maize harvest (Djaman et al, 2022).

ii) options for adaptation and mitigation using genotype analysis

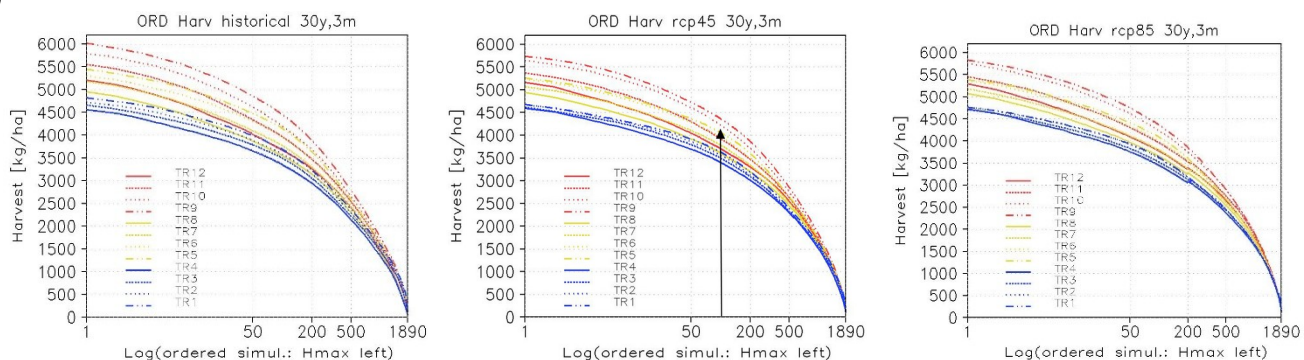
These three features of cross genotype-agro-management impact: - projected lower maxims of H in scenarios (mainly for 520 early sowing), projected higher intermediate H (mainly mid-late sowing); - a narrowing of the range of H in the top and intermediate H-percentile intervals GX and GI with higher/ lower expectancy of intermediate/ high values occurrence, have practical adaptation outcomes.

Finding mitigation solutions, while preserving yield, e.g. finding appropriate changes in agro-management practice that allows a lower, less pollutant fertilization, at a same Harvest percentile, appears indeed to be supported by genotype selection. Fig. 9 (mitigation window shown for RCP4.5) indicates that for a Harvest given percentile, we get intervals in GI and also in GX where changing the sowing date for a lower fertilization, brings even improved solutions. These intervals are defined by intersection points of H-curves defining parameter-zones of both mitigation and optimisation.

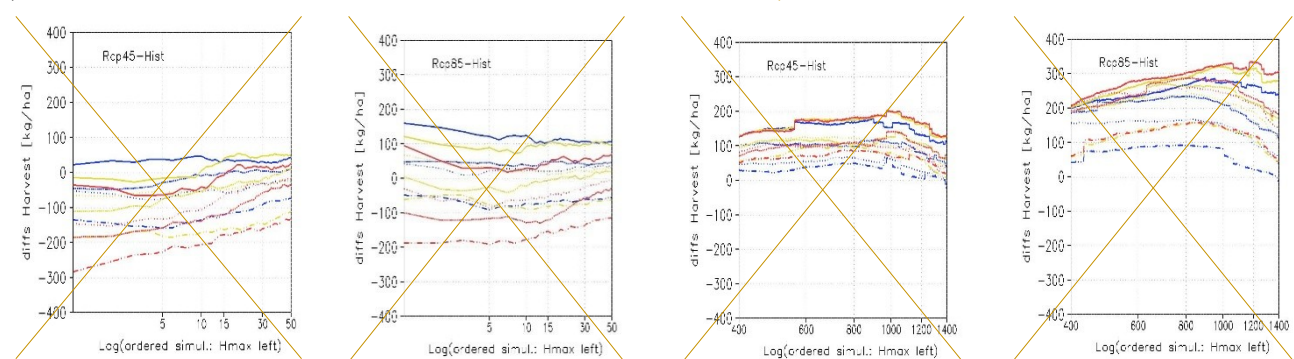
The first two points are equivalent to slopes' change of H as a function of the ordered genotype, as shown in (Supl. S3) in climate scenario versus Hist. Slope change information indicates the percentile (and genotype) threshold for improving the result in scenario compared to Hist, for a given agro-management. Alternatively, for a given H value and treatment, one may estimate the interval of genotype leading that value, information useful to improve local usage.

genotype one could find how a change in management practice could optimize the result. In this last case for example, one could choose a small shift in the sowing, but using less fertilisation, less pollutant, meanwhile getting a same or even higher H, as shown for example in TR5 versus TR11 in Fig.9a, RCP4.5 (Fig.9).

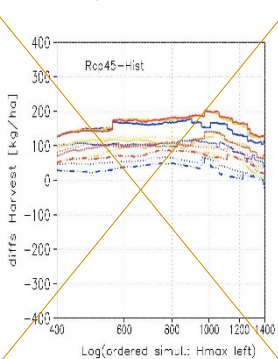
535 a)



b)



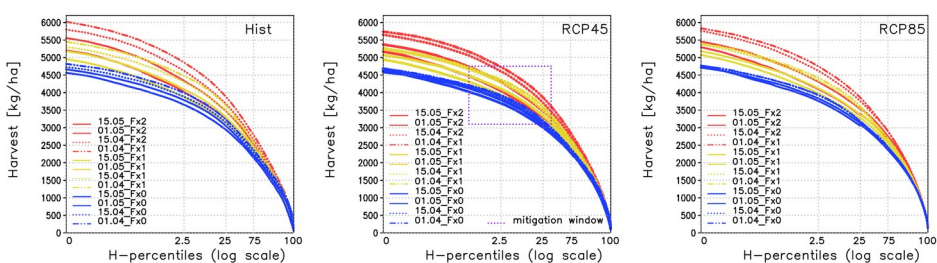
c)



540

545

Fig.9 a): Harvest multi-model time mean, ordered from maximum to minimum value (left to right on x-axis, logarithmic scale). The simulations are for: Hist (left), RCP4.5 (middle) and RCP8.5 (right), experiment setup E_1N_Gn+w, for cross-genotype changes in six Pi parameters (resulting 1890 simulations, x-axis); b) differences in projected harvest for a) RCP4.5 minus Hist (left) and RCP8.5 minus Hist (right), for the upper H percentile (the first 50 values, [1-50] on x axis) and intermediate in c), range [400-1400] on x-axis. ("Hmax left" indicates that increasing values of H are on leftward direction of the axis).



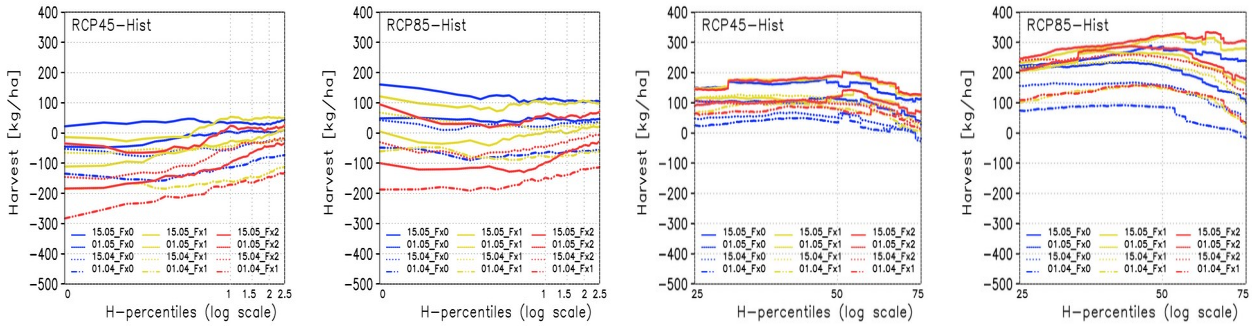
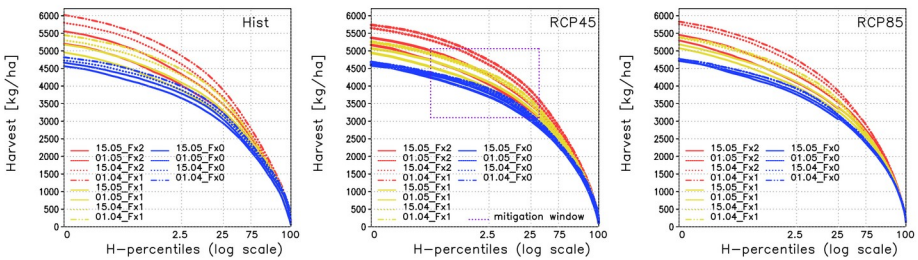


Fig.7 a): Harvest multi-model time mean: percentiles of the H distribution ordered from maximum to minimum value (left to right on x-axis, logarithmic scale). The simulations are for: Hist (left), RCP4.5 (middle) and RCP8.5 (right) for multi-parameter genotype changes (for six parameters resulting 1890 simulations); b) differences in projected harvest for a) RCP4.5 minus Hist (left) and RCP8.5 minus Hist (right), for the upper H 2.5 percentile (the first 50 values) and intermediate in c), percentile 25%-75% (475-1400) on x-axis. Plum rectangle in Fig.7b (RCP4.5) shows in simulations, a window of potential actions for mitigation through genotype- agro-management selection (text).

Apart from any comparison with Hist, it is important for long term adaptation, that one may find genetic combinations with high yield in specific target percentile under a given climate (e.g. first 50 values, as in Fig.9Fig.7b).

At yearly level, the interest for some of these genotype parameters combinations may increase, providing that distinct 590 weather favourable patterns will be identified, once with progress achieved in seasonal and annual weather forecasting (Dewitte et al., 2021).

3.3.2 Optimal Genotype parameters P_i under climate change

i) optimal genotype parameters

We further discriminate H response per genotype parameters (P1-P56), to understand the source of the changes in Fig.9Fig.7 595 and the possible adaptation paths under climate and management scenarios.

Parameters' analysis (Fig. 10) shows that in all simulations, higher harvest is obtained under: shorter thermal time from seedling to juvenile phase (P1, Fig. 10 a), shorter photoperiod-delay (P2, Fig.10Fig.8b), slightly shorter thermal time between successive leaves appearance (phyllochron, P56, Fig. 10 e) in the intermediate H-percentile interval G1 and longer in the top one GX, but longer thermal time to maturity (P3, Fig.10Fig.8c) and higher grain filling rate (P45, Fig. 10d). These 600 results are in coherence with findings along recent works. Shorter P1 or lowering the seedling-juvenile thermal time for increasing H (Fig. 10a) is in agreement with Mi et al., (2021) for semi-humid areas, (the current class of this region, with semi-arid trends projected, Fig. 4), and the same for P2, while slower maturity (P3) and enhanced filling rate (P45) being linked to higher kernel weight and harvest in agreement with recent studies (Grewer et al., 2024).

ii) changes in optimal genotype parameters in climate scenarios

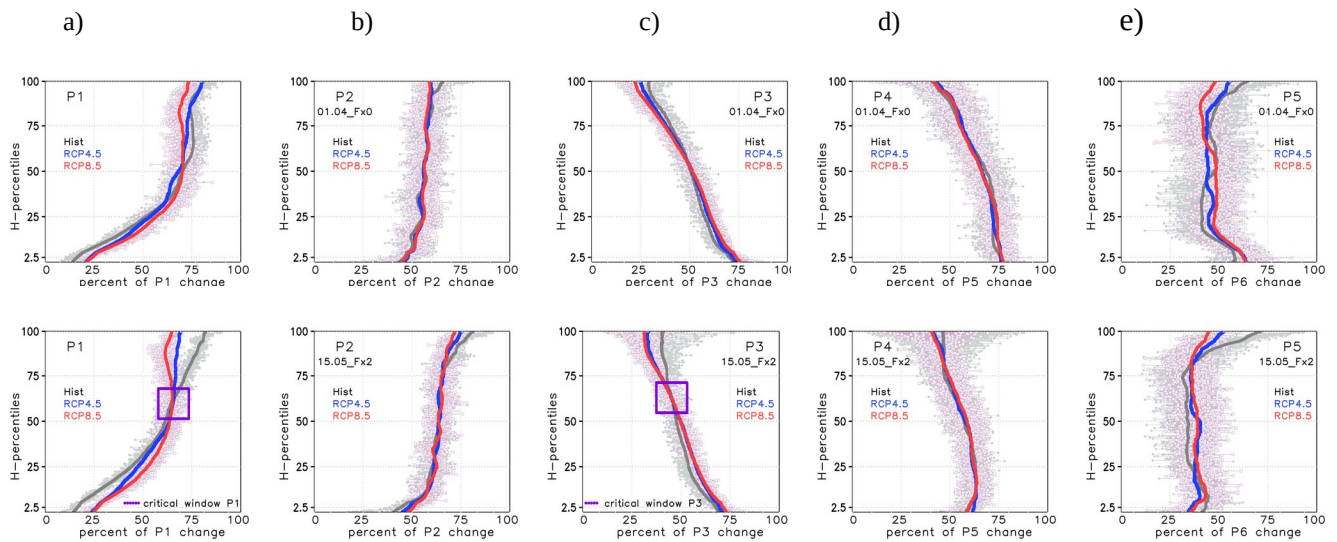
605 Comparing the genotype parameters P_i in climate scenarios against Hist, reveals the new plant strategy put in place in the new climatic conditions, for maximizing the harvest. The ensemble simulations (Fig. 10) shows that highest harvests are reached with genotypes that ensure a longer thermal time from seedling to juvenile phase and longer thermal time to maturity in scenarios compared to Hist. To a smaller extent this is also achieved by a longer photoperiod delay P2, higher grain filling rate P4 and longer phyllochron interval P5, in scenarios, than for a same percentile of the Harvest in Hist. These 610 show that under warmer climate it is essentially important to avoid too fast growth on vegetative and grain filling main stages of the development.

Indeed, slower development phases are obtained in scenarios mainly by increasing P1 and P3 (Fig.10Fig.8a, b) and related to these, under longer photoperiod (P2 increases, Fig.10Fig.8b). Other contributions come from ensuring a slower rate of appearance of successive leaves (P45 increase), while a higher grain filling rate (P56 increase) appears to partly compensate

615 for the negative effect of higher temperature that decreases the seed-filling duration and seeds number and size and finally the harvest.

In other studies, this compensation was shown to be minor compared to the loss of seed-filling duration in warmer climate (Singh et al., 2013) that points to P1 and P3 as main drivers for Harvest in climate scenarios. Percentages of the parameters' Pi changes in scenarios versus Hist for a given percentile of harvest (suppl. S44) confirm this main driving.

620



635

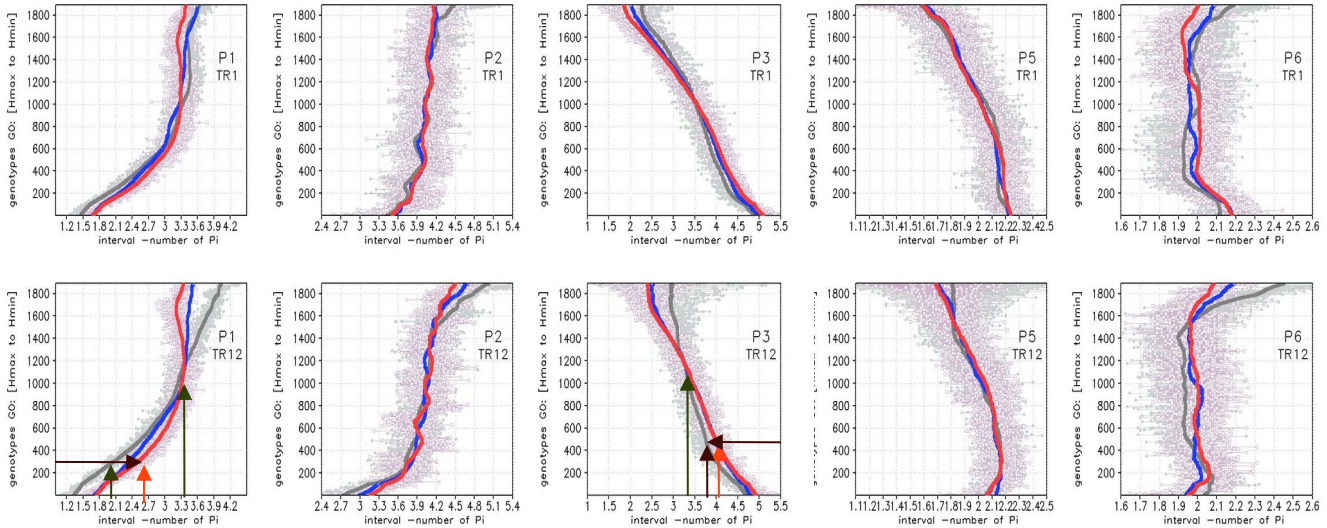


Fig.8: Parameters' i values corresponding to percentiles of the H distribution (ordered from maximum to minimum value). On Ox is the percent of parameter change relative to the interval tested for each, normalised to its control value, ordered, decreasing harvest (on y axis, the number of the ordered simulation, $y=1$ is the highest harvest simulation). The figure compares these percentiles for Hist (black), RCP4.5 (blue) and RCP8.5 (red), running mean values, ensemble mean, time-mean (full lines, 100 values window); unsmoothed values are shown by dots only for Hist and RCP8.5, RCP4.5 being intermediate in all cases). Percentiles are from a number of 1890 genotype simulations. X-axis shows the Pi interval-number of discretization, increasing with increased values. Discretization here have used $5 \times 7 \times 6 \times 1 \times 3 \times 3$ intervals for $P1 \times P2 \times P3 \times P4 \times P5 \times P6$ (total 1890). These are Simulations are shown for two treatments (01.04_Fx0TR1 at top and 15.05_Fx2TR12 at bottom), for: Hist (black), RCP4.5 (blue, only shown for the running mean) and RCP8.5 (red), ensemble time-mean; full lines show running means over 100 values window. The short arrows in a) and c) indicate, for a same harvest percentile ($y=$ constant) the corresponding Pi intervals for Hist (black) and RCP8.5 (red); long arrows indicate the $P0i$ values of the intersection of running-mean Pi for Hist with RCP8.5. The plum rectangle indicates a critical parameter value for P1 and P3 (text), threshold that controls when the scenario leads better/ worse H values that Hist in scenario simulations here.

iii) optimal genotype parameters in management and climate scenarios

Agro-treatments choice may significantly modulate the H response to genotype parameters. Delaying sowing, requires gradually decreasing parameter_i in order to maximize H (Fig.11Fig.9, also in Fig.10Fig.8), for both Hist and climate scenarios. For P1-P3 this decrease reflects the priority in avoiding a too late end of the juvenile stage (and shift in climate conditions) and a too late (autumn) maturity stage that is slowing the grain filling and leading crop failure.

However, Fig. 11 also shows that these parameter_i decreases cease or even reverse under extreme delay of sowing. For highest delays the development stage is getting too short under P1's too strong decrease while daily temperatures becoming higher, hampering the development. The same is seen for the maturity, with P3' too strong decrease favouring a too quick grain filling. Hence the plant strategy for adaptation after a threshold of sowing-delay is similar to the one already seen in its adaptation to warmer climate, in scenarios. Higher harvest is then reached by gradually switching to only moderate decrease or even increases of P_i -parameters along with gradual increasing delays in the sowing date.

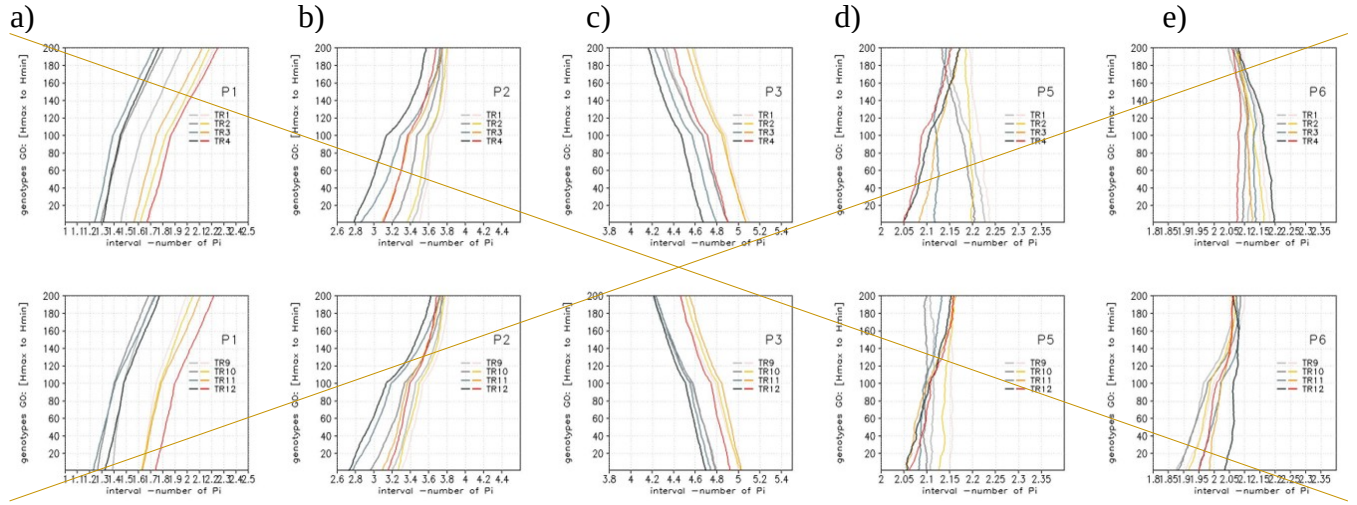
This gradual switch in the mechanism of parameters_i performing high harvest, with sowing delay appears quite systematic for all parameters_i . This crop adaptation mechanism, converging to the one projected for climate scenarios, shows that

gradually under enhanced warming, the crucial priority in adaptation transfers, from the key issue of ensuring climatological

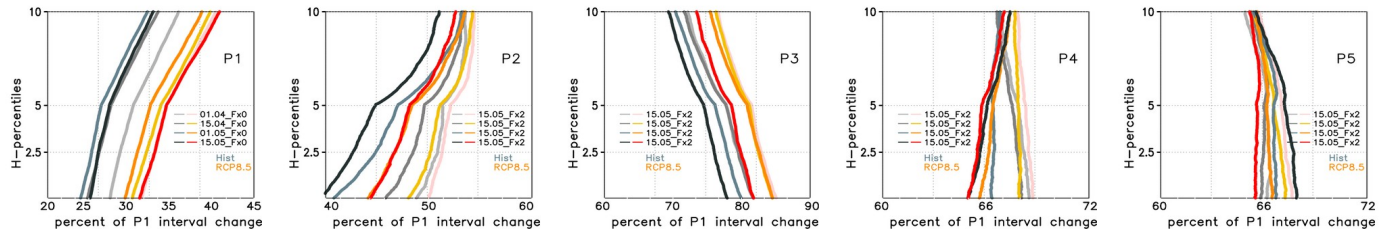
665 conditions for the development to the key issue of avoiding a too fast growth leading crop failure.

This gradual change of switch in the monotony along mechanism of parameters P_i performing high harvest, with sowing delay appears quite systematic for all P_i parameters. This crop adaptation mechanism towards the $-$ converging to the one-one found in projections for climate scenarios, shows that gradually under enhanced warming, the main crucial priority in adaptation, transfers, from the key constraint issue of ensuring climatological conditions for the development to the key issue of avoiding a too fast growth and leading crop failure.

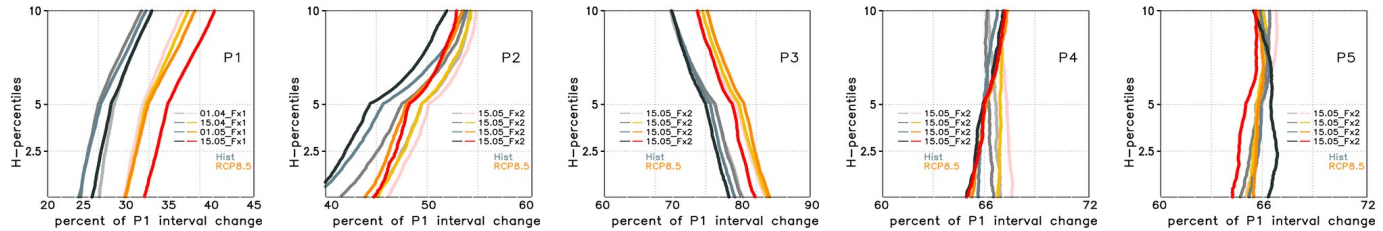
670



675



680



685

Fig.11 Fig.9 As in Fig.10 Fig.8 but for all sowing dates, no fertilization Fx0 (TR1-4, top) and with fertilization Fx2 (TR9-12, bottom). Parameters P_i are shown for the top 10% 200 highest harvest (from 1 to 400). On O_x is the percent of parameter change relative to the interval tested for each. Grey colours are for Hist and yellow-red for RCP8.5 (light to dark is from earlier to latest sowing).

iv) optimal genotype parameters in adaptation and mitigation strategy

690 For each agro-management and climate scenario one can identify threshold values of parameters P_i (critical window shown in Fig.8 for P1 and P3 at the intersection between scenario and Hist) P_{0i} that depend on the parameter P_i , the sowing date and the fertilization level, shown in Fig.10Fig.8 of intersection between scenario and Hist. When reaching At this parameter value, for the genotypes leads the same H-percentile the two have the same H percentile. So this value (critical parameter on Fig.8, P1 and P3) P_{0i} shows the value for which the advantage brought by shortening (P1) and/or decreasing (P3) in scenarios compared to Hist, information useful for adaptation under climate scenarios.

695 if we get an enhanced percentile or decreased from genotypes with higher or lower P_i in the scenario compared to Hist (Fig.10Fig.8, shown by arrows).

Second remark is on the expectancy of an outcome. Since all the slopes of P_i , each as a function of H ordered-values are lower than in Hist (suppl. S53), there is a narrower P_i interval for all those P_i decreasing with 700 H (e.g. P1) and a border one for those P_i increasing with H (P3, Fig.10Fig.8c), in climate scenarios. P3 increases are broadening the interval for H-highest percentile, potentially presenting, in this sense, more expectancy (than P1, Fig.10Fig.8a) on highest values outcome.

The genotyping results were found both in simulations involving deterministic and the hybrid deterministic-ML methods. The hybrid method involved the same cross-simulations, but the selection of P_i values for H optimization and 705 ordering was no more following a pre-defined discretisation but instead a random picking up over a continuous interval of values with successively retrieving the best generation. It applies for optimization, classic Genetic Algorithms methods in which selection of pairs is based on the user-criteria (e.g. maximum harvest, stable harvest, etc.). Our results show that for the same physical intervals of the genotype parameters, the ML hybrid technique only after 20 generations shows at least 50% chances to get a better result than the deterministic model, while after 100 generations, it already increases at 80% 710 chances to get better results with also computational efficiency. CPU time is reduced in this case by more than 30% using the hybrid technique compared to the fully deterministic model on a VM Linux platform. Hybrid method emerges as a better solution since it can identify improved optimums at lower computational prices.

4. Discussions

The results found are in line with other results in recent studies, using different approaches and observational data, and offer 715 an extended (continuum-parameter) assessment towards a more generalised frame, allowed by the implemented system. For the plant response under management treatment delaying sowing date, limiting elongations of the development phase was also found in other studies (Huang et al., 2020) to reduce the impact of temperature increase and, in some cases, precipitation decrease and water stress. This response was also found stronger under enhanced fertilization and delayed sowing (Fig. 10, 11). Also fertilization lowering P56 and enhancing leaf appearance rate (Fig. 10f), assessed in earlier studies mainly for

720 warmer climates (Hokmalipour et al., 2011; Sardans et al., 2017; dos Santos et al., 2021) was recently put in relation to P2 decrease mainly along sensitive photoperiods (Hu et al., 2023) and to higher harvest, through enhanced evapo-transpiration maximizing the high N uptake (Lu et al., 2024). In warmer climate scenarios ([Fig.10](#)[Fig.8f](#), [Fig.9](#)[f](#)), limitations in the expansion of new leaves (increase of P56, [Fig.10](#)[Fig.8](#)) was shown to be an adaptive tolerance mechanism to drought and heat stress conditions (Fahad et al., 2017).

725 | Further, for moderate sowing delay fertilisation was shown to require slower grain filling (P45, [Fig.11](#)[Fig.9d](#)) under reduced P1, P2 and P3, controlling N stimulated growth under hydric stress conditions of current and projected climate for non-irrigated crop (Yang et al., 2024). Under high delay and warmer climate, a higher grain filling is required ([Fig.11](#)[Fig.9d](#)). This increase for P45 under increased warming may reflect an adaptive strategy of plants to accelerate development under drought stress, allowing plants to end their life cycle before impact of severe drought stress occurs (McKay et al., 2003; 730 Roeber et al., 2022).

Simulations here emphasize and compare adaptation paths of gradual plant response to warming climate. These emphasise some reduction in the efficiency of adaptation through crop management in warmer climates. Meanwhile, genotyping shows the possibility of identifying parameters still able to enhance efficiency of adaptation under climate and agro-management scenarios, hence suitable methods for an accelerating change. The ability of exploring continuum-parameter space not only 735 offers a general picture of adaptation cross-solutions but identifies critical values of the parameters that for small perturbations may lead the system response into different states (threshold sowing-delays, or P0i for genotypes). Without an integrated modelling approach, estimating or emphasising these points meaningful for adaptation is hard, moreover since these are simulation (climate-management scenario) dependent.

5. Conclusions

740 The main outcome of this study is that an agroclimatic real-time Interactive Service was implemented towards adaptation support, that allows performing real-time, user-requested, agro-management modelling scenarios for the region, under current and future climate. A novel feature of the system is the ability for identifying optimal management paths for the user's request, along with multiple cross-cultivar parameters, such as cross-optimal sowing date, genotype parameters, amount and date of fertilization.

745 The system provides solutions and estimates the associated uncertainty by using multi-model ensembles for each agro-climate and management scenario. The crop optimization criteria are user-defined and can relate to high harvest, stable harvest, low pollution. The optimization module implemented uses a hybrid deterministic - ML methodology. It performs multi-model simulations using physical models of climate and plant penology and optimization is done either through discretizing the parameters' space and optimisation post-processing or using hybrid physical-ML Genetic Algorithms 750 methods. ML methods are spanning continuous parameter's space and iteratively selecting along the simulations the best fit parameters, allowing to identify unprecedented optimal configurations (H maxims), not reachable under the discrete

deterministic method. The overall system output information is layered and accessed from two interfaces: one static, for information purpose (phenology, harvest, climate, extremes at high resolution NUTS3 level) and a second is real-time interactive online, through which the user places requests and receives the system-performed management simulations required (including uncertainty along multi-models) and identified optimal paths for adaptation. These platforms are operational for two emission scenarios RCP4.5 and RCP8.5 and twelve management scenarios (sowing dates and fertilization), for the time-horizon up to 2050, with open-source code (EERIS platform). The results of these were discussed in this work for the pilot region South Romania.

For the current genotype, in both emission scenarios it is projected a mean decrease (14% in ensemble mean, with higher values per model) of the projected harvest, for all the management scenarios (sowing-dates and fertilization) tested. This was linked to a projected shortening of the grain filling season (10% quicker with an earlier shift of both anthesis (5 day) and maturity (10 day) phases) and to a mean decrease of the fertilisation efficiency under climatic scenarios, stronger in RCP 8.5 emissions.

The impact of genotype perturbations on crop parameters is analysed along six cross-genotype parameters, for agro-management-climate scenarios. The main questions: i) Can we identify optimal genotype parameters that lead to maximal harvest? How do these differ under projected climate change and/ or under agro-management options and can these enhance our understanding to guide our options? iii) Can be genotyping a (better) solution for adaptation under climate change in the region?

These simulations showed that the maximal H values are projected to decline for all agro-management and breeding simulations performed, in emission scenarios compared to Hist, with a higher decline for earlier sowing. H-values then increase in the intermediate-percentile harvest in scenarios versus Hist and there is enhanced expectancy in scenarios to reach the historical values in this range through agro-management and breeding. These indicate a narrowing of the responses range to same agro-managements, with less / more expectancy of reaching values in the highest / intermediate H-range of Hist, in climate scenarios. In practice, these express that we can identify the H-percentile (genotype), where agro-management choice will optimize the outcome compared to Hist, including finding solutions with lower fertilisation, less pollutant.

| For effective support in adaptation applications, individual genotype parameters P_i were analysed in climate scenarios versus Hist. This showed that the thermal times to juvenile (P1) and maturity (P3) are key genotype parameters driving harvest changes in the region, requiring increased values in climate scenarios compared to Hist for a same highest harvest-percentile range. This range is identified through critical values of the parameters (P01), determined for each treatment and climate scenario. There is significant variability of P0i under agro-management treatments. Moderate delayed sowing and enhanced fertilisation may diminish the shifts in parameters_P in scenarios compared to Hist for a same H-percentile, in contrast to extreme managements.

These results show that Genetic approaches offer adaptation strategy support in helping plants to resist drought stress under warming climate. Moreover, it was shown that the optimization is improved by using a hybrid ML genetic

algorithm method coupled to the deterministic model-output, leading to detecting better solutions, under a continuous-parameter space search. The system can be further used for searching paths along extreme drought years, along with irrigation options investigation. Coupled with weather extended predictions (seasonal, year -decadal) this could provide near real-time adaptation support.

790

Code and data availability: The code is available in the Github repository at: <https://github.com/pneague/Genetic-Algorithm-for-Corn-Genotype-sowing-Date-Optimization> under a BSD 2-Clause Simplified License

795

Author contribution: MC: model implementation, code for optimal adaptation tool, pre and post-processing, model simulations, results analysis, development of the User-Platform, paper writing; LC: DSSAT model set-up, results analysis, paper review; PN: ML method implementation and runs, results analysis, paper writing; AD: model validation; VA: development of the Info-Platform; ZC and AI: platforms upload and update; AP: agro-meteorological station data providing; GC: DSSAT model input for the target region.

800

Competing interests: The contact author has declared that none of the authors has any competing interests

Acknowledgments: The authors are grateful to UEFISCDI who provided the financial support of this work under the Project Grant PREPCLIM PN-III-P2-2.1-PED-2019-5302.

805

References

810

1. Adams, R. M., Hurd, B. H., Lenhart, S., & Leary, N. (1998): Effects of global climate change on agriculture: an interpretative review. **Climate Research**, 11(1), 19–30.
2. Angus, J.F., Mackenzie, D.H., Morton, R., & Schafer, C.A. (1981): Phasic development in field crops II. Thermal and photoperiodic responses of spring wheat, **Field Crops Research**, 4, 269-283, ISSN 0378-4290, [https://doi.org/10.1016/0378-4290\(81\)90078-2](https://doi.org/10.1016/0378-4290(81)90078-2).
3. Arnell, N.W., & Freeman, A. (2021): The effect of climate change on agro-climatic indicators in the UK. **Climatic Change**, 165, 40, <https://doi.org/10.1007/s10584-021-03054-8>.
4. Asseng, S., Ewert, F., Martre, P., Rötter, R. P., Lobell, D., Cammarano, D., Kimball, B., et al. (2015): Rising temperatures reduce global wheat production. **Nature Climate Change**, 5.
5. Baez-Gonzalez, A. D., Kiniry, J., Maas, S., et al. (2005): Large-Area Maize harvest Forecasting Using Leaf Area Index Based harvest Model. **Agronomy Journal**, 97. 10.2134/agronj2005.0418.
6. Bai, Y., Yue, W., & Ding, C. (2021): Optimize the Irrigation and Fertilizer Schedules by Combining DSSAT and GA.

7. Baltas, E. (2007) Spatial Distribution of Climatic Indices in Northern Greece. *Meteorological Applications*, 14, 69-78. [www.interscience.wiley.com <http://dx.doi.org/10.1002/met.7>](http://dx.doi.org/10.1002/met.7)

820 8. Banterng, P., A. Patanothai, K. Pannangpatch, S. Jogloy, and G. Hoogenboom. 2004. Determination of genetic coefficients of peanut lines for breeding applications, *European Journal of Agronomy* 21(3):297-310.

9. Basso, B., Shuai, G., Zhang, J., et al. (2019): harvest stability analysis reveals sources of large-scale nitrogen loss from the US Midwest. *Sci Rep*, 9, 5774, <https://doi.org/10.1038/s41598-019-42271-1>.

10. Benestad, R., Buonomo, E., Gutiérrez, J.M., et al. (2021): Guidance for EURO-CORDEX climate projections data use, 825 Version 1.1.

11. Bernardo, R. (2002): *Breeding for Quantitative Traits in Plants*. Stemma Press, 9780972072403, <https://books.google.ro/books?id=3T2FQgAACAAJ>.

12. Berti, A., Maucieri, C., Bonamano, A., & Borin, M. (2019): Short-term climate change effects on maize phenological phases in northeast Italy. *Italian Journal of Agronomy*, DOI: 10.4081/ija.2019.1362.

830 13. Birch, C.J., Vos, J., Kiniry, J., Bos, H.J., & Elings, A. (1998): Phyllochron responds to acclimation to temperature and irradiance in maize, *Field Crops Research*, 59(3), 187-200, ISSN 0378-4290, [https://doi.org/10.1016/S0378-4290\(98\)00120-8](https://doi.org/10.1016/S0378-4290(98)00120-8).

14. Boogaard, H., Wolf, J., Supit, I., Niemeyer, S., & van Ittersum, M. (2013): A regional implementation of WOFOST for calculating harvest gaps of autumn-sown wheat across the European Union, *Field Crops Research*, 143, 130-142, ISSN 835 0378-4290, <https://doi.org/10.1016/j.fcr.2012.11.005>.

15. Caian, M., Georgescu, F., Pietrisi, M., & Catrina, O. (2021): Recent Changes in Storm Track over the Southeast Europe: A Mechanism for Changes in Extreme Cyclone Variability. *Atmosphere*, 12(10):1362. <https://doi.org/10.3390/atmos12101362>

16. Caian, M.; Andrei, M.D. Late-Spring Severe Blizzard Events over Eastern Romania: A Conceptual Model of 840 Development. *Atmosphere* 2019, *10*, 770. <https://doi.org/10.3390/atmos10120770>

17. Ceglar, A., Zampieri, M., Gonzalez-Reviriego, N., et al. (n.d.): Time-varying impact of climate on maize and wheat harvests in France since 1900. *Environmental Research Letters*, 15(9), <https://doi.org/10.1088/1748-9326/aba1be>.

18. Chang, Y., Latham, J., Licht, M. et al. A data-driven crop model for maize yield prediction. *Commun Biol* 6, 439 (2023). <https://doi.org/10.1038/s42003-023-04833-y>

845 19. Chapagain, R., Remenyi, T. A., Huth, N., Mohammed, C. L., & Ojeda, J. J. (2023): Investigating the effects of APSIM model configuration on model outputs across different environments. *Frontiers in Agronomy*, <https://www.frontiersin.org/articles/10.3389/fagro.2023.1213074>

20. Chazarreta, Y. D., Amas, J. I., & Otegui, M. E. (2021): Kernel filling and desiccation in temperate maize: Breeding and environmental effects, *Field Crops Research*, 271, 108243, ISSN 0378-4290, <https://doi.org/10.1016/j.fcr.2021.108243>.

850 21. Chen, Y., & Tao, F. (2022): Potential of remote sensing data-crop model assimilation and seasonal weather forecasts for early-season crop yield forecasting over a large area, **Field Crops Research**, 276, 108398, ISSN 0378-4290, <https://doi.org/10.1016/j.fcr.2021.108398>.

22. Cooper, M., & Messina, C. D. (2023): Breeding crops for drought-affected environments and improved climate resilience, **The Plant Cell**, 35(1), 162–186, <https://doi.org/10.1093/plcell/koac321>.

855 23. Dainelli, R., Calmanti, S., Pasqui, M., et al. (2022): Machine learning for regional crop harvest forecasting in Europe, **Field Crops Research**, 276, 108377, ISSN 0378-4290, <https://doi.org/10.1016/j.fcr.2021.108377>.

24. Djaman K., Samuel Allen, Dorlote S. Djaman, Komlan Koudahe, Suat Irmak, Naveen Puppala, Murali K. Darapuneni, Sangamesh V. Angadi, Planting date and plant density effects on maize growth, yield and water use efficiency, **Environmental Challenges**, 6, 2022, 100417, ISSN 2667-0100, <https://doi.org/10.1016/j.envc.2021.100417>

860 25. dos Santos, C. L., et al. (2022): Maize Leaf Appearance Rates: A Synthesis From the United States Corn Belt. *Frontiers in Plant Science*, 13, <https://doi.org/10.3389/fpls.2022.872738>.

26. Espadafor, M., Orgaz, F., Testi, L., et al. (2017): Responses of transpiration and transpiration efficiency of almond trees to moderate water deficits, *Scientia Horticulturae*, 225, 6-14, ISSN 0304-4238, <https://doi.org/10.1016/j.scienta.2017.06.028>.

865 27. Eyring, V., Mishra, V., Griffith, G.P., et al. (2021): Reflections and projections on a decade of climate science. *Nature Climate Change*, 11(4), 279-285.

28. Fahad, et al. (2017): Crop Production under Drought and Heat Stress: Plant Responses and Management Options. *Frontiers in Plant Science*, 8, <https://doi.org/10.3389/fpls.2017.01147>.

29. Flocas, A. A. *Courses of meteorology and climatology*. Ziti Publications: Thessaloniki (1994)

870 30. Ganguly, 2013: Post harvest losses of agricultural produce. *International Journal of Agricultural Sciences*, 9(2), June, 2013 , 818-820

31. Godfray, H., Charles, J., et al. (2010): Food Security: The Challenge of Feeding 9 Billion People. *Science*, 327, 812-818.

32. Grewer, U., Kim, D.-H., & Waha, K. (2024): Too much, too soon? Early-maturing maize varieties as drought escape strategy in Malawi, *Food Policy*, 129, 102766, ISSN 0306-9192, <https://doi.org/10.1016/j.foodpol.2024.102766>.

875 33. Hatfield, J.L., et al. (2020): Indicators of climate change in agricultural systems. *Climatic Change*, 163, 1719–1732.

34. Hoogenboom, G., Porter, C.H., Sheila, V., Boote, K. J., Singh, U., White, J. W., Hunt, L.A., Ogochi, R., Lizaso, J.I., Koo, J., Asseng, S., Singels, A., Moreno, L.P. and Jones, J. W. 2019. Decision Support System for Agrotechnology Transfer (DSSAT) Version 4.7. DSSAT Foundation

35. Hokmalipour, S. (2011): The Study of Phyllochron and Leaf Appearance Rate in Three Cultivar of Maize (*Zea mays L.*) At Nitrogen Fertilizer Levels. *Agricultural and Food Sciences*.

880 36. Huang, M., et al. (2020): *Environmental Research Letters*, 15, 024015; DOI 10.1088/1748-9326/ab66ca

37. Huang N, Xiaomao Lin, Fei Lun, Ruiyun Zeng, Gretchen F. Sassenrath, Zhihua Pan, Nitrogen fertilizer use and climate interactions: Implications for maize yields in Kansas, *Agricultural Systems*, Volume 220, 2024, 104079, ISSN 0308-521X, <https://doi.org/10.1016/j.agsy.2024.104079>

885 38. Hu, H., et al. (2023): The effects of photoperiod and temperature-related factors on maize leaf number and leaf positional distribution in the field. *Frontiers in Plant Science*, 14, <https://doi.org/10.3389/fpls.2023.1006245>.

39. IPCC, 2022 *Climate Change 2022: Impacts, Adaptation and Vulnerability*. IPCC Sixth Assessment Report

40. Jin, X., Jin, Y., Zhai, J., et al. (2022): Identification and prediction of crop Waterlogging Risk Areas under the impact of climate change. *Water*, 14, 1-21, 10.3390/w14121956.

890 41. Jones, J., Hoogenboom, G., Porter, C., et al. (2003): The DSSAT cropping system model. *European Journal of Agronomy*, 18, 235-265, [https://doi.org/10.1016/S1161-0301\(02\)00107-7](https://doi.org/10.1016/S1161-0301(02)00107-7).

42. Kakar, K.M., Khan, A., Khan, I., et al. (2014): Growth and yield response of maize (*Zea mays L.*) to foliar NPK-fertilizers under moisture stress condition. *Soil and Environment*, 33(2),

43. Khan, F. , Khan, S. , Fahad, S. , Faisal, S. , Hussain, S. , Ali, S. and Ali, A. (2014) Effect of Different Levels of Nitrogen and Phosphorus on the Phenology and Yield of Maize Varieties. *American Journal of Plant Sciences*, 5, 2582-2590. doi: 10.4236/ajps.2014.517272.

895 44. Karl E. Taylor, Ronald J. Stouffer, Gerald A. Meehl, A summary of the CMIP5 Experiment Design, 2011

45. Kothari, K., Ale, S., Marek, G.W., Munster, C.L., Singh, V.P., Chen, Y., Marek, T.H., & Xue, Q. (2022): Simulating the climate change impacts and evaluating potential adaptation strategies for irrigated corn production in Northern High Plains of Texas, *Climate Risk Management*, 37, 100446, ISSN 2212-0963, <https://doi.org/10.1016/j.crm.2022.100446>

900 46. Langworthy, A. D., et al. (2018): Potential of summer-active temperate (C 3) perennial forages to mitigate the detrimental effects of supraoptimal temperatures on summer home-grown feed production in south-eastern Australian dairying regions. *Crop Pasture Sci.*, 69, 808-820.

47. Lelieveld, J., Hadjinicolaou, P., Kostopoulou, E., et al. (2012): Climate change and impacts in the Eastern Mediterranean and the Middle East. *Climatic Change*, 114, 667-687, <https://doi.org/10.1007/s10584-012-0418-4>.

905 48. Li, M., & Tang, Y. (2022): Climate warming causes changes in wheat phenological development that benefit yield in the Sichuan Basin of China, *European Journal of Agronomy*, 139, 126574, ISSN 1161-0301, <https://doi.org/10.1016/j.eja.2022.126574>

49. Liu, K., Harrison, M.T., Yan, H., et al. (2023): Silver lining to a climate crisis in multiple prospects for alleviating crop waterlogging under future climates. *Nature Communications*, 14(1), 765, 10.1038/s41467-023-36129-4.

910 50. Liu, K., et al. (2020): Identifying optimal sowing and flowering periods for barley in Australia: a modelling approach. *Agric. For. Meteorol.*, 282-283, 107871.

51. Lu, J., Stomph, T.J., Mi, G., et al. (2024): Identifying and quantifying the contribution of maize plant traits to nitrogen uptake and use through plant modelling, *in silico Plants*, 6(2), diae018, <https://doi.org/10.1093/insilicoplants/diae018>.

915 52. Malhi, G.S.; Kaur, M.; Kaushik, P. Impact of Climate Change on Agriculture and Its Mitigation Strategies: A Review. *Sustainability* 2021, 13, 1318. <https://doi.org/10.3390/su13031318>

53. Mamassi, A., Balaghi, R., Devkota, K.P., et al. (2023): Modelling genotype × environment × management interactions for a sustainable intensification under rainfed wheat cropping system in Morocco. *Agriculture and Food Security*.

54. Marcinkowski, P., & Piniewski, M. (2018): Effect of climate change on sowing and harvest dates of spring barley and

920 maize in Poland. *International Agrophysics*, 32(2), 265-27

55. Meehl, G.A., Stocker, T.F., Collins, W.D., et al. (2007): Global Climate Projections. In: Solomon, S., Qin, D., Manning, M., et al. (Eds.), Cambridge University Press.

56. Meroni M, François Waldner, Lorenzo Seguini, Hervé Kerdiles, Felix Rembold, Yield forecasting with machine learning and small data: What gains for grains?, *Agricultural and Forest Meteorology*, Volumes 308–309, 2021, 108555, ISSN 0168-925 1923, <https://doi.org/10.1016/j.agrformet.2021.108555>

57. Mi, N.; Cai, F.; Zhang, S.; et al. (2021): Thermal Time Requirements for Maize Growth in Northeast China and Their Effects on Yield and Water Supply under Climate Change Conditions. *Water*, 13, 2612. <https://doi.org/10.3390/w13192612>

58. Mitchell, R.J., Bellamy, P.E., Broome, A., et al.: Cumulative impact assessments of multiple host species loss from plant diseases show disproportionate reductions in associated biodiversity. *Journal of Ecology*, <https://doi.org/10.1111/1365-2745.13798>.

930 59. McKay, J. K., Richards, J. H., & Mitchell, T. (2003). Genetics of drought adaptation in *Arabidopsis thaliana*: I. Pleiotropy contributes to genetic correlations among ecological traits. *Molecular ecology*, 2003

60. McKee, T.B.; Doesken, N.J.; Kleist, J. (1993): The Relationship of Drought Frequency and Duration to Time Scales. In Proceedings of the Eighth Conference on Applied Climatology, Anaheim, CA, USA, 17–22 January 1993; pp. 179–184.

935 61. Morales, A., & Villalobos, F. (2023): Using machine learning for crop harvest prediction in the past or the future. *Frontiers in Plant Science*, 14, 1128388, 10.3389/fpls.2023.1128388.

62. Morell, F-J., Yang, H.S., Cassman, K.G., et al. (2016): Can crop simulation models be used to predict local to regional maize harvests and total production in the U.S. Corn Belt? *Field Crops Research*, 192, 1-12, ISSN 0378-4290, <https://doi.org/10.1016/j.fcr.2016.04.004>.

940 63. Patra Abhik, Vinod Kumar Sharma, Dhruba Jyoti Nath, Asik Dutta, Tapan Jyoti Purakayastha, Sarvendra Kumar, Mandira Barman, Kapil Atmaram Chobhe, Chaitanya Prasad Nath & Chiranjeev Kumawat (2022): Long-term impact of integrated nutrient management on sustainable harvest index of rice and soil quality under acidic inceptisol, *Archives of Agronomy and Soil Science*, DOI: 10.1080/03650340.2022.2056597.

64. Paudel, Allard de Wit, Hendrik Boogaard, Diego Marcos, Sjoukje Osinga, Ioannis N. Athanasiadis, Interpretability of

945 deep learning models for crop yield forecasting, *Computers and Electronics in Agriculture*, Volume 206, 2023, 107663, ISSN 0168-1699, <https://doi.org/10.1016/j.compag.2023.107663>

65. Peleman, J-D., & Rouppe van der Voort, J. (2003): Breeding by Design, *Trends in Plant Science*, 8(7), 330-334, ISSN 1360-1385, [https://doi.org/10.1016/S1360-1385\(03\)00134-1](https://doi.org/10.1016/S1360-1385(03)00134-1).

950 66. Pfeiffer, W., & McClafferty, B. (2007): HarvestPlus: Breeding Crops for Better Nutrition. *Crop Science*, 47. [10.2135/cropsci2007.09.0020IPBS](https://doi.org/10.2135/cropsci2007.09.0020IPBS).

67. Popescu A., Dinu T.A, Stoian E, Servan V, 2021, the use of chemical fertilizers in Romania's agriculture. *Scientific Papers. Series "Management, Economic Engineering in Agriculture and rural development"*, Vol. 21 ISSUE 4, PRINT ISSN 2284-7995, 469-476.

687. Qiao, L., Xiaojun, Z., Li, X., et al. (2022): Genetic incorporation of genes for the optimal plant architecture in common wheat. *Molecular Breeding*, 42, 10.1007/s11032-022-01336-2.

68. Rezaei, E.E., Webber, H., Asseng, S., et al. (2023): Climate change impacts on crop harvests. *Nature Reviews Earth and Environment*.

698. Roeber, V., Schmulling T, Cortleven A., (2022): The Photoperiod: Handling and Causing Stress in Plants *Frontiers in Plant Science*, 12, [<https://doi.org/10.3389/fpls.2021.781988>](<https://doi.org/10.3389/fpls.2021.781>

960 7069. Rosenzweig, C., Jones, J.W., Hatfield, J.L., et al. (2013): The Agricultural Model Intercomparison and Improvement Project (AgMIP): Protocols and pilot studies. *Agricultural and Forest Meteorology*, 170, 166-182, <https://doi.org/10.1016/j.agrformet.2012.09.011>.

710. Sardans, J., Grau, O., Chen, H.Y.H., et al.: Changes in nutrient concentrations of leaves and roots in response to global change factors. *Global Change Biology*, <https://doi.org/10.1111/gcb.13721>.

965 724. Schauberger, B., Jägermeyr, J., & Gornott, C. (2020): A systematic review of local to regional harvest forecasting approaches and frequently used data resources. *European Journal of Agronomy*, 120, 126153, <https://doi.org/10.1016/j.eja.2020.126153>.

732. Schwalbert , R., Amado , T.,Nieto , L. et al. (2020). Mid-season county-level corn yield forecast for US Corn Belt integrating satellite imagery and weather variables. *Crop Sci.* 60 : 739 – 750

970 743. Selvaraju, R., et al. (2011): Climate science in support of sustainable agriculture and food security. *Climatic Research*, 47, 95–110.

754. Semenov, M., & Stratonovitch, P. (2015): Adapting wheat ideotypes for climate change: Accounting for uncertainties in CMIP5 climate projections. *Climate Research*, 65. 10.3354/cr01297.

765. Shaw, T.A., & Miyawaki, O. (2024): Fast upper-level jet stream winds get faster under climate change. *Nature Climate Change*, 14, 61–67. <https://doi.org/10.1038/s41558-023-01884-1>

776. Simmons, A. (2021): The ERA-Interim archive Version 2.0, ERA Report Series.

787. Singh R.P, P. V. Vara Prasad, K. Raja Reddy, Chapter Two - Impacts of Changing Climate and Climate Variability on Seed Production and Seed Industry,Editor(s): Donald L. Sparks,Advances in Agronomy,Academic Press,Volume 118,2013,Pages 49-110,ISSN 0065-2113,ISBN 9780124059429,<https://doi.org/10.1016/B978-0-12-405942-9.00002-5>

980 798. Smil, V. 2005. The next 50 years: Unfolding trends. *Population and Development Review* 31: 605-643.

8079. Stehr, N., & von Storch, H. (2000): Climate and society: climate as resource, climate as risk. *World Scientific*.

810. Su, Z., Liu, Z., Bai, F., et al. (2021): Cultivar selection can increase yield potential and resource use efficiency of spring maize to adapt to climate change in Northeast China. *Journal of Integrative Agriculture*, 20(2): 371–382.

824. Tao, F., Zhao, Z., Liu, J., & Yokozawa, M Modelling the impacts of weather and climate variability on crop
985 productivity over a large area: A new super-ensemble-based probabilistic projection.

832. Tsvetsinskaya, E.A., Mearns, L.O., & Easterling, W.E. (2002): Investigating the Effect of Seasonal Plant Growth and Development in Three-Dimensional Atmospheric Simulations. Part I: Simulation of Surface Fluxes over the Growing Season. [[https://doi.org/10.1175/1520-0442\(2001\)014](https://doi.org/10.1175/1520-0442(2001)014)]

843. Tsimba R, Gregory O. Edmeades, James P. Millner, & Peter D. Kemp (2013): The effect of planting date on maize: 990 Phenology, thermal time durations and growth rates in a cool temperate climate, Field Crops Research, 150, 145-155, ISSN 0378-4290, <https://doi.org/10.1016/j.fcr.2013.05.021>.

854. Trnka, M., et al. (2014): Adverse weather conditions for European wheat production will become more frequent with climate change. Nature Climate Change, 4, 637–643.

86. Ursu A., Efficiency of chemical fertilizer use in Romanian agriculture. Comparative study based on FAOSAT data, 995 *ULST Timisoara, Multidisciplinary Conference on Sustainable Development 15-16 May 2025*

875. Villalobos, F., Pérez-Priego, O., Testi, L., et al. (2012): Effects of water supply on carbon and water exchange of olive trees. European Journal of Agronomy, 40, 1-7. 10.1016/j.eja.2012.02.004.

886. van Ittersum M., Kenneth G. Cassman, Patricio Grassini, Joost Wolf, Pablo Tittonell, Zvi Hochman, Yield gap analysis with local to global relevance—A review, Field Crops Research, Volume 143, 2013, Pages 4-17, ISSN 0378- 1000 4290, <https://doi.org/10.1016/j.fcr.2012.09.009>

897. Yang Y. , Jiabo Yin, Shengyu Kang, Louise J. Slater, Xihui Gu, Aliaksandr Volchak, Quantifying the drivers of terrestrial drought and water stress impacts on carbon uptake in China, Agricultural and Forest Meteorology, Volume 344, 2024, 109817, ISSN 0168-1923, <https://doi.org/10.1016/j.agrformet.2023.109817>

908. Wang, Y., Jiang, K., Shen, H., et al. (2023): Decision-making method for maize irrigation in supplementary irrigation 1005 areas based on the DSSAT model and a genetic algorithm. Agricultural Water Management, 280, 108231.

9189. Webber, H., Ewert, F., Olesen, J.E., et al. (2018a): Diverging importance of drought stress for maize and winter wheat in Europe. Nature Communications, 9(1), 1-11. 10.1038/s41467-018-06525-2.

920. Webber, H., et al. (2020): Pan-European multi-crop model ensemble simulations of wheat and grain maize under climate change scenarios, Open Data Journal for Agricultural Research, 6, 21-27.

1010 | 934. Wheeler, T., & von Braun, J. (2013): Climate change impacts on global food security. Science, 341(6145), 508-13. 10.1126/science.1239402.

942. World Development Report 2008: Agriculture for Development.

953. Wu J-Z, Jing ZHANG, Zhang-ming GE, et al. (2021): Impact of climate change on maize harvest in China from 1979 to 2016, Journal of Integrative Agriculture, 20(1), 289-299, ISSN 2095-3119, [https://doi.org/10.1016/S2095-3119\(20\)63244-0](https://doi.org/10.1016/S2095-3119(20)63244-0).

1015 | 964. Xie, W., Zhu, A., Ali, T., et al. (2023): Crop switching can enhance environmental sustainability and farmer incomes in China. Nature, 616, 300–305. <https://doi.org/10.1038/s>.

| 975. Xu Honggen, Bo Ming, Keru Wang, et al. (2023): Quantitative analysis of maize leaf collar appearance rates, Plant Physiology and Biochemistry, 196, 454-462, ISSN 0981-9428, <https://doi.org/10.1016/j.plaphy.2023.01.016>.

| 986. Zhuang H, Zhao Zhang, Fei Cheng, Jichong Han, Yuchuan Luo, Liangliang Zhang, Juan Cao, Jing Zhang, Bangke He,
1020 Jialu Xu, Fulu Tao, Integrating data assimilation, crop model, and machine learning for winter wheat yield forecasting in the
North China Plain, Agricultural and Forest Meteorology, Volume 347, 2024, 109909, ISSN 0168-1923,
<https://doi.org/10.1016/j.agrformet.2024.109909>

1025 | **Annex: Data and Methods: Steps in ML algorithm**

| Schema of steps in workflow of ML algorithms for optimal genotype identification:

| **Start with 10 randomly chosen solutions within the bounds of P1-P6;**

| Calculate the mean and std of harvest of each solution for the 30 years 1976-2005;

| Calculate fitness = (Mean of harvest) - (Standard deviation of Harvest/4);

1030 | Randomly choose 4 pairs of 'parents', with the probability being chosen weighted by the fitness;

| For each pair of parents A and B, create identical children 'a' and 'b' to the parents, then choose a random number of P's to be subjected to crossover, called x;

| For each child, modify Px as follows:

| $P_{xa} = \text{round}(B * P_{xa} + (1 - B) * P_{xb})$

1035 | $P_{xb} = \text{round}((1 - B) * P_{xa} + B * P_{xb})$

| Where P_{xa} is the value of the x parameter of child "a" (initially identical to that of parent A), and B is the blending factor, set in this paper to 0.75. This technique is called blending, and it generates offspring chromosomes that inherit real-valued traits from both parents while exploring the search space between the parents' positions. The blending crossover promotes a smoother and more gradual search for optimal solutions in continuous domains.

1040 | Then take each child, and with a probability of 0.5 perform a mutation on one of its chromosomes. This means setting one of the P's to a random value between its allowed minimum and maximum.

| At this point the children have been fully constructed. Discard the 8 parents with the lowest fitness and substitute them with the children.

| **Repeat:**

1045 | **Supplementary material:**

| S1: Simulated (ERA5 control runs) versus measured harvest

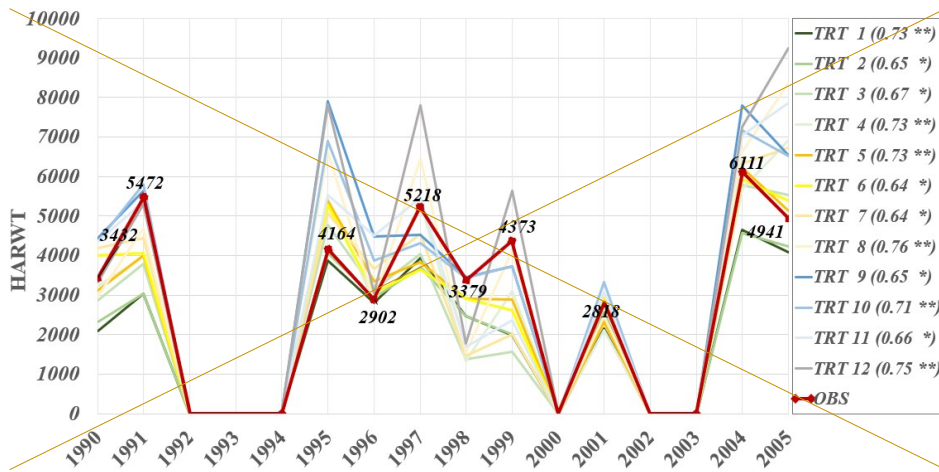
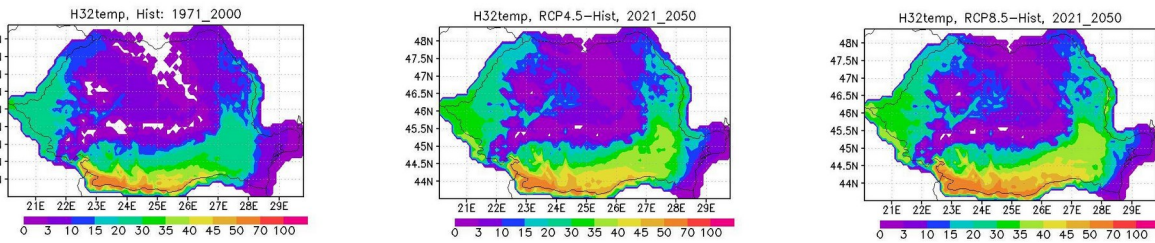


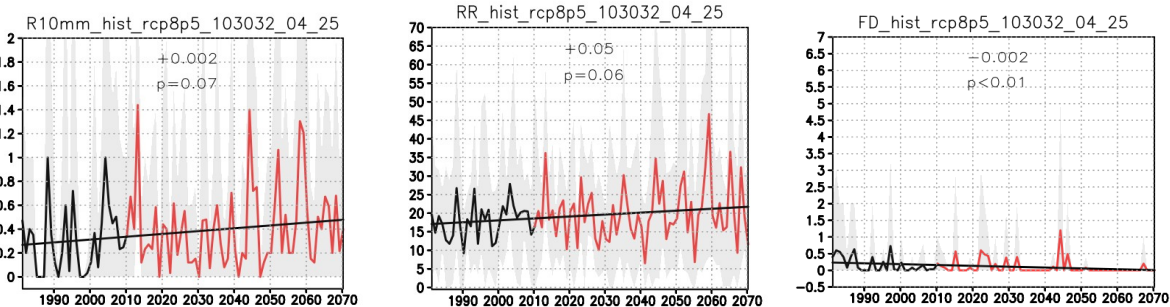
Fig.S1: Simulated (thin lines) vs. measured (red, thick) harvest in southern Romania for 12 management scenarios (Table 1, expt "3N"). Box: Pearson correlation between simulated treatments and measured Harvest (** p<0.01, ** p<0.05, * p<0.10; zero are missing values).

S1: Projected changes in agro-climate indicators over the SE Romania

a)



b)



S.1 a): The scorching index H32temp (degrees above 32C in summer JJA) for: Hist (1971-2000) and changes (2021-2050) relative to it, under RCP4.5 (middle) and RCP8.5 (right). The scorching index classes are: reduced intensity drought for $H32temp \in [0, 10]$, moderate intensity for $H32temp \in (10, 30]$, high intensity for $H32temp \in (30, 50]$ and severe drought conditions for $H32temp > 50$.

b): Climate parameters (NUTS region 103032 Ilfov county, representative for the target region), along historical (Hist) and RCP8.5 scenarios; a): RR10, the number of days with heavy precipitation (>10 mm per day) in a 10-day period; b): RR, total

precipitation (mm) per 10-day period; (left): the 10-day period is centred on April 5th; (right): the 10-day period is centred on April 25th ; c). FD, the number of frost days (minimum temperature < 0°C in a 10-day period). Values indicate the slope of the linear trend (black line) and the p-value of significance (p-values < 0.05 are statistically significant at the 5% level).

S2: Sensitivity to changes in nutrients

Replicability for system portability on other pilot regions requires estimates of sensitivity to new local forcing. Sensitivity ensemble simulations were performed, with increasing soil Carbon and Nitrogen at the initial time by 20%, for a same control genotype (experiment setup E_1N_G0_soil+CN).

a) b) c)

Fig.S2.1: Harvest (kg/ha) comparison between the experiment setup E_3N_G0 (top, same as Fig.7 Fig.5) and the experiment setup E_1N_G0_soil+CN (bottom). Panels are as in Fig7, for Fx0(a), Fx1 (b), Fx2 (c), ensemble time mean for Hist (black), RCP4.5 (green) and RCP8.5 (red), on Ox there is the treatment (1 to 12, Table 1).

Experiment E_1N_G0_soil+CN compared to E_3N_G0 (Fig.7 Fig.5) shows that Harvest loss is only up to 7% for about 60% reduction in fertilization (exper “1N” versus “3N”, Table 1), when the soil nutrients content is increased by 20%. Also, the comparison shows that there are still options even under warmer climate to equal or exceed the historical Harvest if there is an appropriate soil composition (e.g. in RCP4.5 TR6 and TR7, Fig.S2.1b-bottom), also under RCP8.5 (TR10 and TR11, Fig.S2.1c-bottom), and even at lower fertilization levels (exp “1N”, Table 1). A possible mechanism in this case involves delayed maturity (Fig.S2.2b), and consequent more precipitation accumulated (Fig.S2.2a, c). In practice this slower maturity could be due to soil C/N composition influencing soil water holding capacity, moisture and temperature, slowing germination or plant growth. Previous research (Kakar et al. 2014; Khan et al., 2014) also reported delayed silking and maturity in the case of enhanced soil nitrogen when compared to control case, showing also a stronger response for early sowing.

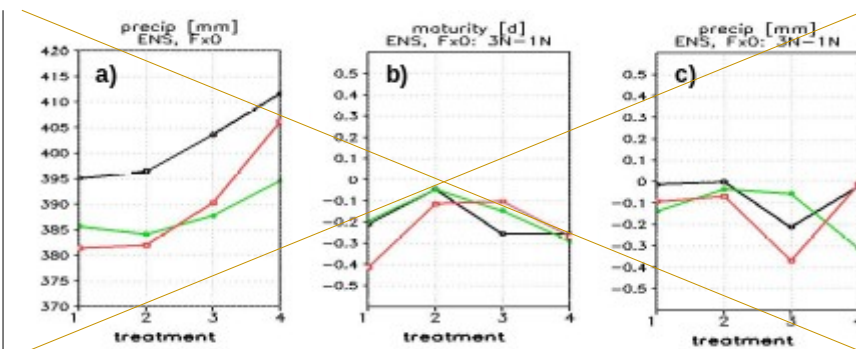


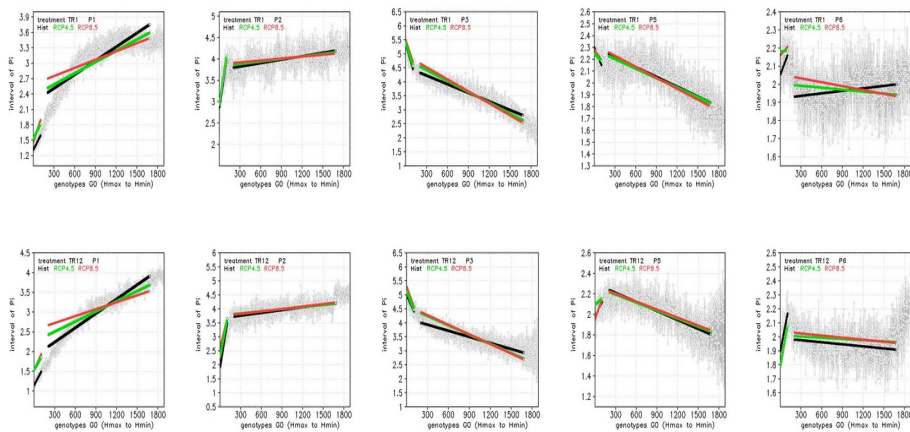
Fig.S2.2: Precipitation (mm) accumulated from the initial time of the simulation for experiment setup E_3N_G0 (a), (same as Fig.7), differences [dap] in the maturity date (b) and in precipitation accumulated until maturity (c) for the experiment

setup E_3N_G0 minus the experiment setup E_1N_G0_soil+CN, (mm). Lines are for Hist (black), RCP4.5 (green) and RCP8.5 (red).

S2: Harvest as a function of fertilization and precipitation

1095 | S3: Model-spread for optimal genotype

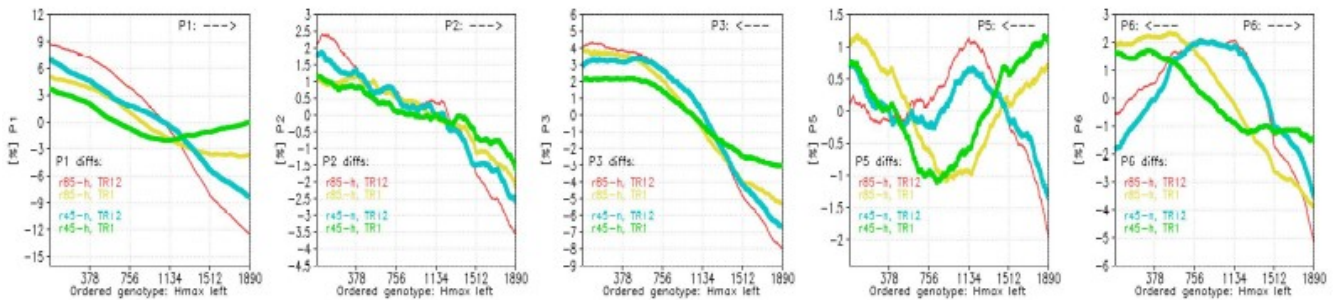
S3: Slopes of Pi genotype parameters in Hist and climate scenarios



1100 Fig.S3 The slopes (thick lines) of Pi genotype parameters (y-axis) as a function of decreasing ordered harvest (x-axis) for Hist (black), RCP4.5 (green and RCP8.5 (red) computed over 2 sub-intervals of highest 200 values of harvest and over the rest of decreasing ordered values (200-1890). The values (light grey) are plot for Hist, ensemble time mean, TR12 (as in Fig.10Fig.8 bottom, grey).

1105

S44: Percent changes in Pi in climate scenarios relative to Hist

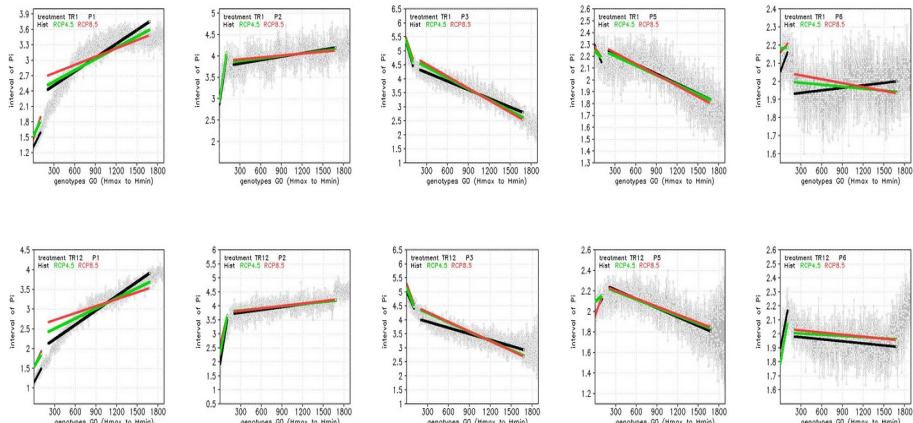


1110

Fig.S4: Percent changes of Pi genotype parameters (y-axis) as a function of the ordered Harvest from highest (left, x-axis) to lowest (right, x-axis). Differences (running means over $378 = P2 \times P3 \times P4 \times P5 \times P6$ the product of discretization intervals for P1-P56) are shown for TR1 (yellow for RCP4.5 minus Hist) and green (RCP4.5 minus Hist) and for TR12 (red for RCP8.5 minus Hist) and blue (for RCP4.5 minus Hist). Percent changes are expressed as differences relative to Hist. Arrows indicate the monotony of Pi values that correspond to the ordered decreasing harvest (shown in Fig.10 Fig.8).

1115

S5: Slopes of Pi genotype parameters in Hist and climate scenarios



1120

Fig.S3 The slopes (thick lines) of Pi genotype parameters (y-axis) as a function of decreasing ordered harvest (x-axis) for Hist (black), RCP4.5 (green and RCP8.5 (red) computed over 2 sub-intervals of highest 200 values of harvest and over the rest of decreasing ordered values (200-1890). The values (light grey) are plot for Hist, ensemble time mean, TR12 (as in Fig.8 bottom, grey).

1125